Dalton Transactions

ROYAL SOCIETY OF CHEMISTRY

PAPER

View Article Online
View Journal | View Issue

Check for updates

Cite this: *Dalton Trans.*, 2022, **51**, 7142

Synthesis and reactivity of an iridium complex based on a tridentate aminophosphano ligand†

Marco Palmese, Jesús J. Pérez-Torrente and Vincenzo Passarelli *

The iridium(III) hydride compound [IrH{κ^3*C,P,P*′-(SiNP–H)}(CN^tBu)$_2$][PF_6] (**1**PF_6) was obtained by reaction of [Ir(SiNP)(cod)][PF_6] with CN^tBu as the result of the intramolecular oxidative addition of the $SiCH_2$–H bond to iridium(I) [SiNP = $Si(CH_3)_2${N(4-tolyl)PPh_2}$_2$, SiNP–H = $CH_2Si(CH_3)${N(4-tolyl)PPh_2}$_2$]. The mechanism of the reaction was investigated by NMR spectroscopy and DFT calculations showing that the penta-coordinated intermediate [Ir(SiNP)(cod)(CN^tBu)][PF_6] (**2**PF_6) forms in the first place and that further reacts with CN^tBu, affording the square planar intermediate [Ir(SiNP)(CN^tBu)$_2$][PF_6] (**3**PF_6) that finally undergoes the intramolecular oxidative addition of the $SiCH_2$–H bond. The reactivity of **1**PF_6 was investigated. On one hand, the reaction of **1**PF_6 with *N*-chlorosuccinimide or *N*-bromosuccinimide provides the haloderivatives [IrX{κ^3*C,P,P*′-(SiNP–H)}(CN^tBu)$_2$][PF_6] (X = Cl, **4**PF_6; Br, **5**PF_6), and the reaction of **5**PF_6 with $AgPF_6$ in the presence of acetonitrile affords the solvato species [Ir{κ^3*C,P,P*′-(SiNP–H)}(CH_3CN)(CN^tBu)$_2$]$^{2+}$ (**6**$^{2+}$) isolated as the hexafluorophosphate salt. On the other hand, the reaction of **1**PF_6 with HBF_4 gives the iridium(III) compound [IrH($CH_2SiF_2CH_3$)(HNP)$_2$(CN^tBu)$_2$][BF_4] (**7**BF_4) as the result of the formal addition of hydrogen fluoride to the Si–N bonds of **1**$^+$ [HNP = HN(4-tolyl)PPh_2]. A similar outcome was observed in the reaction of **1**PF_6 with CF_3COOH rendering **7**PO_2F_2. In this case the intermediate [IrH{κ^2*C,P*-$CH_2SiMeFN$(4-tolyl)PPh_2}(HNP)(CN^tBu)$_2$]$^+$ (**8**$^+$) was observed and characterised *in situ* by NMR spectroscopy. DFT calculations suggests that the reaction goes through the sequential protonation of the nitrogen atom of the Si–N–P moiety followed by the formal addition of fluoride ion to silicon. Also, the crystal structures of SiNP, **1**PF_6, **4**PF_6 and **7**BF_4 have been determined by X-ray diffraction measurements.

Received 14th March 2022,
Accepted 20th April 2022

DOI: 10.1039/d2dt00794k

rsc.li/dalton

Introduction

Aminophosphanes are easily accessible ligands and both nitrogen and phosphorus substituents can be easily varied thanks to the ample diversity of commercially available precursors. So far, aminophosphano ligands of general formula $NHRPR_2$ have been used to prepare mononuclear,[1] di- or oligonuclear species[2] supported by 1κ*N*,2κ*P* aminophosphanes (Fig. 1, top). Alternatively, bidentate aminophosphano ligands have been employed to prepare mononuclear complexes (Fig. 1, bottom).[3–6] In addition, the aminophosphano functionality has been successfully used to decorate ligating functionalities,[7] in some cases as elusive as the silylene[7a,i] and germylene[7a] groups. Remarkably, the applications of these complexes are varied and span catalysis, bond activation, metaloenzyme mimics, drugs, and redox-active multimetallic systems, among others.

Relevant to this paper, in 2001 Woolins reported[5] the synthesis of $SiMe_2${N(2-pyridyl)PPh_2}$_2$ ($SiN^{py}P$) and of its palladium and platinum κ^2*P,P*′-derivatives and thereafter we reported on the preparation of $SiMe_2${N(4-tolyl)PPh_2}$_2$ (SiNP) and its rhodium[6a] and iridium[6b,c] complexes. Notably, beside the expected κ^2*P,P*′ coordination of SiNP, we reported two un-

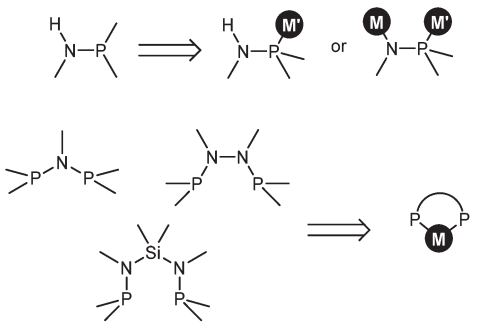

Fig. 1 Selected amino-phosphane scaffolds and related metal–ligand structures.

Departamento de Química Inorgánica, Instituto de Síntesis Química y Catalisis Homogenea (ISQCH), Universidad de Zaragoza-CSIC, C/Pedro Cerbuna 12, ES-50007 Zaragoza, Spain. E-mail: passarel@unizar.es

†Electronic supplementary information (ESI) available: Crystal data, NMR spectra, and atomic coordinates of calculated structures. CCDC 2155640–2155643. For ESI and crystallographic data in CIF or other electronic format see DOI: https://doi.org/10.1039/d2dt00794k

precedented examples[6b,c] of a κ^3C,P,P' coordination of SiNP as a result of the intramolecular $SiCH_2$–H oxidative addition to iridium(I), triggered by π-acceptor ligands such as carbon monoxide or trimethyl phosphite on $[Ir(SiNP)(cod)]^+$ (Scheme 1).

On this background, aiming at further expand the family of metal complexes containing aminophosphano ligands, we decided to assess the capability of *tert*-butyl isocyanide, isoelectronic with CO, to promote the intramolecular $SiCH_2$–H oxidative addition to iridium(I) and eventually explore the reactivity of the resulting complex. So, herein we report on the synthesis of a novel iridium(III) complex of formula $[IrH\{\kappa^3C,P,P'\text{-}(SiNP–H)\}(CN^tBu)_2]^+$ as well as the detailed theoretical and experimental study of the course of its formation. In addition, a reactivity study was carried out on the above mentioned hydrido derivative, including the hydride-halide exchange and the following halide abstraction as well as protonation reactions rendering the unexpected fragmentation of the aminophosphano ligand.

Results and discussion

Synthesis of $[IrH\{\kappa^3C,P,P'\text{-}(SiNP–H)\}(CN^tBu)_2][PF_6]$ (1PF_6)

The reaction of $[Ir(SiNP)(cod)][PF_6]$ with *tert*-butyl isocyanide (1 : 2 molar ratio) yields the hydrido iridium(III) derivative $[IrH\{\kappa^3C,P,P'\text{-}(SiNP–H)\}(CN^tBu)_2][PF_6]$ (1PF_6) (room temperature, 24 h) as a result of the intramolecular $SiCH_2$–H oxidative addition to the metal centre along with the substitution of the cod ligand with two *tert*-butyl isocyanide ligands (SiNP–H = $CH_2SiMe\{N(4\text{-tolyl})PPh_2\}_2$) (Scheme 2).

The crystal structure of 1PF_6 was determined by single crystal X-ray diffraction measurements, and Fig. 2-top shows the ORTEP plot of the cation $[IrH\{\kappa^3C,P,P'\text{-}(SiNP–H)\}(CN^tBu)_2]^+$ (1$^+$). For the sake of comparison, the crystal structure of SiNP was also determined (Fig. 2-bottom). The metal centre of 1$^+$ exhibits an octahedral environment, the metalated κ^3C,P,P'-(SiNP–H) ligand occupying three mutually *cis* coordination sites [C1–Ir–P2 82.79(9)°, P1–Ir–P2 97.00(3)°, C1–Ir–P1 84.83 (9)°]. The hydrido ligand lies *cis* to P1 and *trans* to P2 [P1–Ir–H 87.6(16)°, P2–Ir–H 169.2(16)°]. The remaining coordination sites are occupied by two mutually *cis* isocyanide ligands [C47–Ir–C41 86.18(13)°], one *trans* to P1 [C47–Ir–P1 169.51(10)°] and the other *trans* to the metallated carbon atom C1 [C41–Ir–C1 175.56(13)°]. Reasonably as a consequence of the metalation,

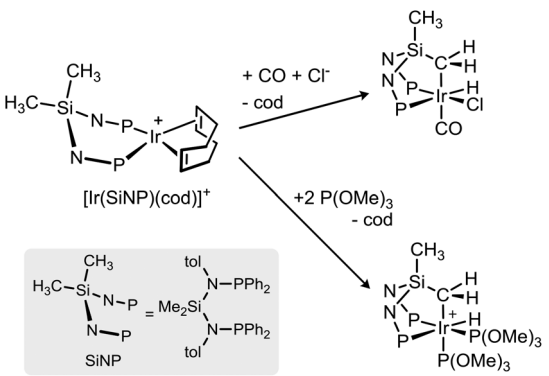

Scheme 1 Reactivity of $[Ir(SiNP)(cod)]^+$ towards CO or $P(OMe)_3$.

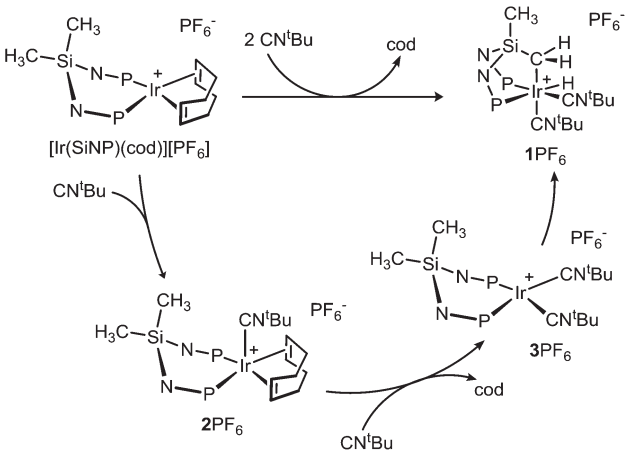

Scheme 2 Reaction of $[Ir(SiNP)(cod)]^+$ with CN^tBu showing the observed intermediates.

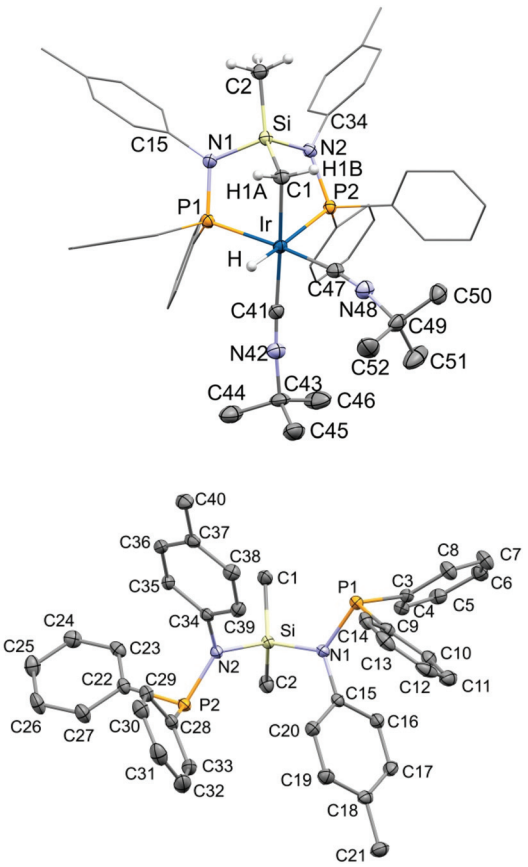

Fig. 2 ORTEP plots of $[IrH\{\kappa^3C,P,P'\text{-}(SiNP–H)\}(CN^tBu)_2]^+$ (1$^+$) (top) and of SiNP (bottom). For clarity, most hydrogen are omitted and the tolyl and phenyl rings are represented in a wireframe style for $[IrH\{\kappa^3C,P,P'\text{-}(SiNP–H)\}(CN^tBu)_2]^+$. Selected bond lengths (Å) and angles (°) are given in ESI.†

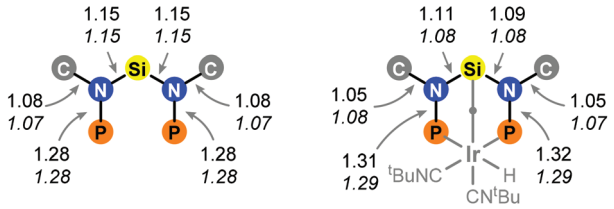

Fig. 3 Selected delocalization indexes (DI) for SiNP and $\mathbf{1}^+$ (normal type, values for the X-ray structure; italic type, values for the DFT-calculated structure).

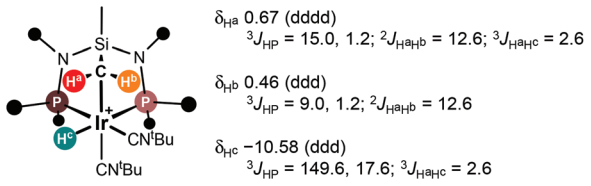

Fig. 4 Selected ^{1}H and ^{31}P NMR data for the IrHCH$_2$ moiety of $\mathbf{1}^+$.

the C1–Si–C2 angle of $\mathbf{1}^+$ [C1–Si–C2 124.65(15)°] is wider than the C1–Si–C2 angle of SiNP [C1–Si–C2 111.48(10)°]. Also, the formation of two fused five member metalacycles in $\mathbf{1}^+$ should account for the smaller Si–N–P angles of $\mathbf{1}^+$ [P2–N2–Si 114.31(15)°, P1–N1–Si 112.48(15)°] when compared with SiNP [P1–N1–Si 121.40(9)°, P2–N2–Si 120.94(9)°]. In addition, it is also remarkable that the nitrogen atoms N1 and N2 of both $\mathbf{1}^+$ and SiNP exhibit a planar geometry, *i.e.* the fragments N1–Si–P1–C15 and N2–Si–P2–C34 are almost planar in both $\mathbf{1}^+$ and SiNP suggesting that a p–d(π) backdonation could imply nitrogen and phosphorus and/or silicon. In this connection, it is worth a mention that the tolyl rings attached to N1 and that attached to N2 lie almost perpendicular to the corresponding N1–Si–P1–C15 and N2–Si–P2–C34 planes in $\mathbf{1}^+$ as well as SiNP ($\mathbf{1}^+$, N1 78.5°; N2 85.3°; SiNP, N1 71.5°, N2 72.2°), which rules out the delocalization of the nitrogen lone pair on the aromatic ring as the cause of the above mentioned planarity of the fragments N1–Si–P1–C15 and N2–Si–P2–C34.

As a confirmation, a QTAIM analysis was carried out on both the crystal and the calculated structures of $\mathbf{1}^+$ and SiNP showing that the delocalization index DI (*aka* fuzzy bond orders, FBO) of the bonds at the nitrogen atoms are 1.08–1.11 (N–C), 1.28–1.32 (N–P) and 1.08–1.15 (N–Si) (Fig. 3) pointing at that some p–d(π) backdonation actually should exist mainly between nitrogen and phosphorus and that therefore it should be responsible for the planar geometry of the nitrogen atoms.

The crystal structure of $\mathbf{1}^+$ should be preserved in solution. Indeed, its ^{31}P{^{1}H} NMR spectrum shows two doublets at 40.3 and 34.4 ppm with a $^2J_{PP}$ coupling constant of 20.4 Hz, in agreement with a *cis* arrangement of the two phosphorus atoms. Also, two ^{1}H singlets at 1.37 and 1.20 ppm are indicative of two non-equivalent *tert*-butyl isocyanide ligands. As for the HIrCH$_2$Si moiety, one ^{13}C doublet of doublets at −29.7 ppm ($^2J_{CP}$ = 2.1, 3.7 Hz) and one ^{1}H multiplet (*vide infra*) at −10.58 ppm have been observed. In addition, similar to the related trimethyl phosphito derivative [IrH{κ^3*C*,*P*,*P*′-(SiNP–H)}{P(OCH$_3$)$_3$}$_2$]$^+$,[6b] the coupling pattern (see $^nJ_{XY}$ in Fig. 4) of the IrHCH$_2$ moiety suggests that the conformation observed in the solid state is maintained in solution.‡

The formation of the hydrido iridium(III) derivative $\mathbf{1}^+$ was observed to be stepwise (Scheme 2). As a matter of fact, the formation of $\mathbf{1}^+$ was monitored by NMR spectroscopy at −80 °C showing that [Ir(SiNP)(cod)(CN^{t}Bu)]$^+$ ($\mathbf{2}^+$) forms in the first place and further reacts with CN^{t}Bu upon raising the temperature, rendering the square planar intermediate [Ir(SiNP)(CN^{t}Bu)$_2$]$^+$ ($\mathbf{3}^+$, *vide infra*) which eventually evolves to $\mathbf{1}^+$. As a confirmation, [Ir(SiNP)(cod)(CN^{t}Bu)][PF$_6$] ($\mathbf{2}$PF$_6$) could be prepared in high yield upon reacting [Ir(SiNP)(cod)][PF$_6$] with *tert*-butyl isocyanide (1 : 1 molar ratio) at −80 °C. Furthermore, the reaction of $\mathbf{2}$PF$_6$ with CN^{t}Bu cleanly yielded $\mathbf{1}$PF$_6$ through $\mathbf{3}$PF$_6$. Remarkably, also in this case, $\mathbf{3}^+$ formed along with $\mathbf{1}^+$, which indicates that the formation of $\mathbf{3}^+$ and its conversion into $\mathbf{1}^+$ should exhibit similar activation barriers. $\mathbf{2}$PF$_6$ was fully characterised in solution by means of multinuclear NMR spectroscopy. A ^{31}P{^{1}H} singlet is observed at 41.4 ppm along with one ^{1}H singlet at 2.04 ppm for the two methyl moieties of the tolyl groups, suggesting that the two Si-Ntol-PPh$_2$ arms of $\mathbf{2}^+$ are equivalent. On the contrary, two ^{1}H singlets at 0.56 and −0.21 ppm are observed for the two SiCH$_3$ groups of $\mathbf{2}^+$, which indicates that they are non-equivalent reasonably as a consequence of the coordination of the isocyanide ligand to iridium in [Ir(SiNP)(cod)]$^+$ rendering a distorted square pyramidal geometry at the metal centre (*vide infra* for the DFT calculated structure). As for the cod ligand, broad ^{1}H signals are observed even at −60 °C for the olefinic (3.46 ppm) and aliphatic hydrogen atoms (1.76 ppm), respectively, suggesting that even at that temperature the putatively non-equivalent olefinic CH moieties as well as the methylene hydrogen atoms are exchanging and their signals are averaged.

As far as the intermediate $\mathbf{3}^+$ is concerned, it could be spectroscopically identified§ *in situ* (^{1}H, ^{31}P NMR). Indeed, a ^{31}P{^{1}H} singlet at 53.7 ppm was assigned to its equivalent phosphorus atoms. Accordingly two equivalent tolyl groups as well

‡The hydrido signal was observed as a ^{1}H{^{31}P} doublet due to the scalar coupling of the IrH hydrogen atom to one of the IrCH$_2$ hydrogen atoms ($^3J_{HH}$ = 2.6 Hz). Accordingly, the ^{1}H{^{31}P} signals at 0.46 and 0.67 ppm, assigned to the IrCH2 moiety, are a doublet ($^2J_{HH}$ = 12.6 Hz) and a doublet of doublets ($^2J_{HH}$ = 12.6, $^3J_{HH}$ = 2.6 Hz), respectively. As already discussed for the related hydrido derivative [IrH{κ^3*C*,*P*,*P*′-(SiNP–H)}{P(OCH$_3$)$_3$}$_2$]$^+$,[6b] this pattern is the consequence of the dependence of the $^3J_{HH}$ constant on the H–X–Y–H dihedral angle (*cf.* M. J. Minch, *Concepts Magn. Reson.*, 1994, **6**, 41–56).

§It is worth a mention that in the course of the related reaction of [Ir(SiNP)(cod)][PF$_6$] with P(OCH$_3$)$_3$ the pentacoordinated derivative [Ir(SiNP)(cod){P(OCH$_3$)$_3$}][PF$_6$], analogous to $\mathbf{2}^+$, could not be isolated and was characterised *in situ* whereas the putative square planar complex [Ir(SiNP){P(OCH$_3$)$_3$}$_2$]$^+$, analogous to $\mathbf{3}^+$, could not even be observed and was proposed only based on DFT calculations (see ref. 6*b*).

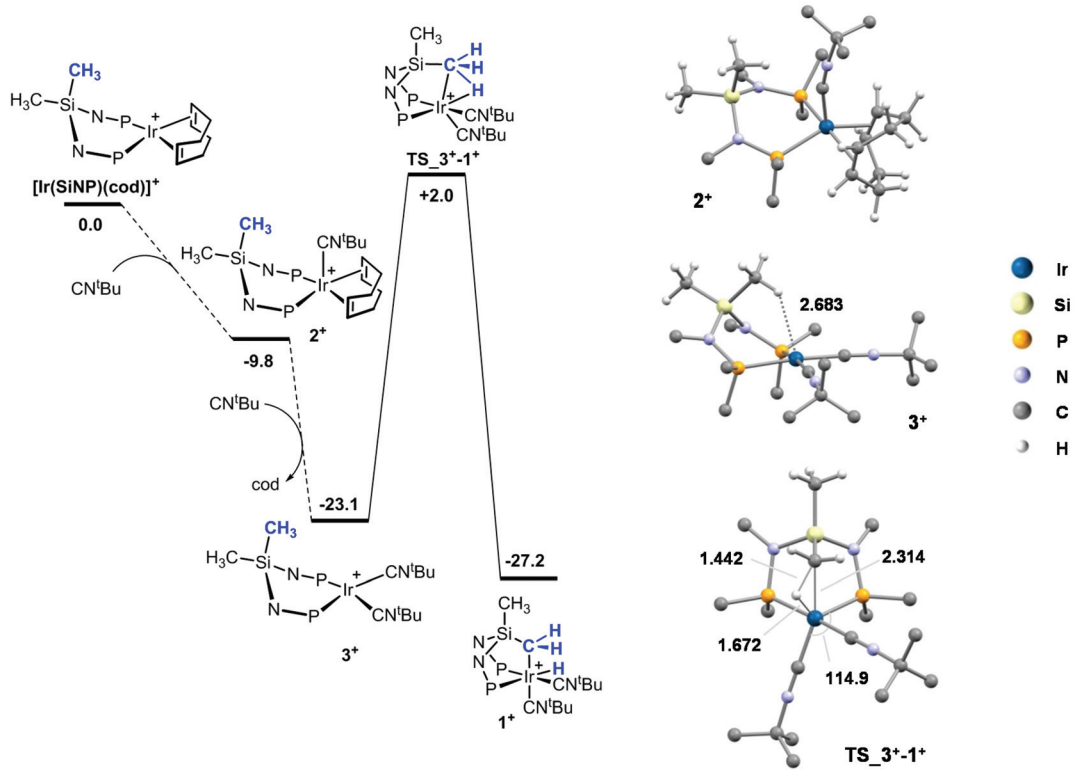

Fig. 5 (left) Relative Gibbs free energy profile (kcal mol^{-1}) of the reaction Ir(SiNP)(cod) + 2 CN^{t}Bu → $\mathbf{1}^+$ + cod (M06/def2tzvp//B3PW91-GD3BJ/def2svp, 298 K, 1 atm); (right) view of the calculated structures of $\mathbf{2}^+$, $\mathbf{3}^+$ and $\mathbf{TS\_3}^+\mathbf{-1}^+$ with selected interatomic distances (Å) and angles (°) (for clarity, most hydrogen atoms are omitted and only the *ipso* carbon atoms of the phenyl and tolyl moieties are shown).

as two equivalent ^{t}Bu and two equivalent SiMe groups were observed.¶

DFT calculations nicely underpinned the proposed pathway for the formation of $\mathbf{1}PF_6$. Fig. 5 shows the simplified Gibbs free energy profile for the reaction Ir(SiNP)(cod) + 2 CN*t*Bu → $\mathbf{1}^+$ + cod, including the calculated structure of the detected intermediates $\mathbf{2}^+$ and $\mathbf{3}^+$ as well as the transition state $\mathbf{TS\_3}^+\mathbf{-1}^+$ of the oxidative addition of $SiCH_2$–H to iridium. The first step is the exoergonic formation of the distorted square pyramidal complex [Ir(SiNP)(cod)(CN^{t}Bu)]$^+$ ($\mathbf{2}^+$). In the following, [Ir(SiNP)(CN^{t}Bu)$_2$]$^+$ ($\mathbf{3}^+$) is obtained by reaction of $\mathbf{1}^+$ with CN^{t}Bu (ΔG_r = −13.3 kcal mol^{-1}). Remarkably $\mathbf{3}^+$ exhibits a boat conformation of the six member ring Ir–P–N–Si–N–P which allows one of the $SiCH_3$ group, namely the flagpole one, to approach the metal centre (CH···Ir 2.683 Å, Fig. 5) and eventually add oxidatively to it ($\mathbf{TS\_3}^+\mathbf{-1}^+$, Fig. 5).

Reactivity of [IrH{κ^3*C*,*P*,*P*′-(SiNP–H)}(CN^{t}Bu)$_2$][PF$_6$] ($\mathbf{1}PF_6$)

In order to assess the applicability of $\mathbf{1}PF_6$ as a catalyst in the functionalization of multiple carbon–carbon bonds, a preliminary reactivity study was undertaken. We observed that $\mathbf{1}PF_6$ does not react either with alkynes – phenylacetylene or 1-hexyne – or alkenes – styrene or 1-hexene – even after prolonged reaction times (up to 48 h) and heating (70 °C in THF). Reasonably the stable κ^3*C*,*P*,*P*′ coordination of the SiNP–H ligand along with the substitutional inertness of the CN^{t}Bu ligands hampered the reactivity of $\mathbf{1}PF_6$. Thus, anticipating that the abstraction of a halido ligand could trigger some reactivity at the Ir{κ^3*C*,*P*,*P*′-(SiNP–H)} platform, we decided to exchange the hydrido ligand with a halido ligand. Thus, the iridium haloderivatives of formula [IrX{κ^3*C*,*P*,*P*′-(SiNP–H)}(CN^{t}Bu)$_2$][PF$_6$] (X = Cl, $\mathbf{4}PF_6$; Br, $\mathbf{5}PF_6$) were prepared by reaction of $\mathbf{1}PF_6$ with *N*-chlorosuccinimide or *N*-bromosuccinimide (Scheme 3).

The crystal structure of $\mathbf{4}PF_6$ was determined by means of X-ray diffraction measurements and it exhibits an octahedral environment of the metal centre with a κ^3*C*,*P*,*P*′-(SiNP–H) ligand along with the chlorido ligand and two *tert*-butyl isocyanide ligands (Fig. 6). The Ir{κ^3*C*,*P*,*P*′-(SiNP–H)} moiety of $\mathbf{4}^+$ and $\mathbf{1}^+$ are virtually superimposable, and by the same token no significant differences are observed between the isocyanide ligands when comparing $\mathbf{1}^+$ and $\mathbf{4}^+$.

The solution structure of $\mathbf{4}^+$ and $\mathbf{5}^+$ should be similar to that of $\mathbf{4}^+$ in the solid state. Indeed, the ^{31}P{^{1}H} NMR spectrum shows two doublets at 28.7 and 26.3 ppm ($\mathbf{4}^+$), and at 25.7 and 25.1 ppm ($\mathbf{5}^+$) with a coupling constant indicating a mutually *cis* disposition of the phosphorus atoms ($^2J_{PP}$ = 18.2 Hz, $\mathbf{4}^+$; 17.4 Hz, $\mathbf{5}^+$). Also, the ^{1}H NMR spectra contains two singlets at

¶Selected ^{1}H NMR data for $\mathbf{3}^+$ (CD_2Cl_2, 298 K) are: δ_H 7.14 (d, $^3J_{HH}$ = 8.1 Hz, 2H, C^{2}H^{tol}), 6.87 (d, $^3J_{HH}$ = 8.1 Hz, 2H, C^{3}H^{tol}), 2.54 (s, 6H, CH$_3^{tol}$), 1.41 ppm (s, 18H, CH$_3^{tBu}$), 0.86 ppm (s, 6H, $SiCH_3$).

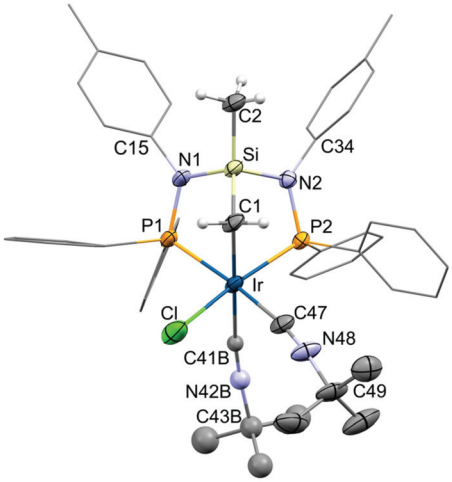

Fig. 6 ORTEP plot of $[IrCl\{\kappa^3C,P,P'\text{-(SiNP–H)}\}(CN^tBu)_2]^+$ ($\mathbf{4}^+$). For clarity, most hydrogen are omitted and the tolyl and phenyl rings are represented in a wireframe style. Selected bond lengths (Å) and angles (°) are given in ESI.†

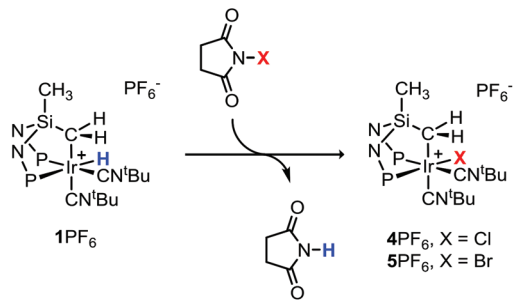

Scheme 3 Hydride-halide exchange on $[IrH\{\kappa^3C,P,P'\text{-(SiNP–H)}\}(CN^tBu)_2][PF_6]$ ($\mathbf{1}PF_6$).

1.45 and 1.25 ($\mathbf{4}^+$), and 1.48 and 1.29 ($\mathbf{5}^+$) ppm for the *tert*-butyl isocyanide ligands, two multiplets at 1.30 and 1.21 ($\mathbf{4}^+$), and 1.37 and 1.24 ($\mathbf{5}^+$) for the $IrCH_2$ moiety, and one singlet at 0.15 ppm ($\mathbf{4}^+$) and 0.17 ppm ($\mathbf{5}^+$) for the $SiCH_3$ group.

The bromido ligand of $\mathbf{5}^+$ was easily abstracted by reaction with $AgPF_6$ but a clean product, namely $[Ir\{\kappa^3C,P,P'\text{-(SiNP–H)}\}(CH_3CN)(CN^tBu)_2][PF_6]_2$ ($\mathbf{6}[PF_6]_2$), could be isolated only in the presence of acetonitrile (Scheme 4), whereas intractable mixtures of products were obtained with styrene or phenylacetylene.

The κ^3C,P,P' coordination of SiNP–H is preserved in $\mathbf{6}^{2+}$ as judged by the $^{31}P\{^1H\}$ doublets observed at 25.1 and 18.0 ppm

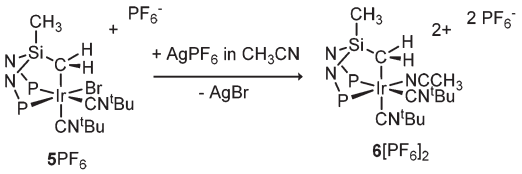

Scheme 4 Bromide abstraction from $[IrBr\{\kappa^3C,P,P'\text{-(SiNP–H)}\}(CN^tBu)_2]^+$ ($\mathbf{5}^+$).

($^2J_{PP}$ = 19.4 Hz) and the ^1H doublet of doublets at 1.44 and 1.30 ppm assigned to the $IrCH_2$ moiety as well as the ^1H singlet at 0.34 ppm for the $SiCH_3$ group. The ^1H singlets at 2.09, 1.48 and 1.29 ppm confirm the presence of one CH_3CN and two CN^tBu ligands, respectively. Unfortunately no reaction of $\mathbf{6}^{2+}$ with either styrene or phenylacetylene was observed indicating that neither CH_3CN nor CN^tBu ligands in $\mathbf{6}^{2+}$ are labile.

Protonation of $[IrH\{\kappa^3C,P,P'\text{-(SiNP–H)}\}(CN^tBu)_2][PF_6]$ ($\mathbf{1}PF_6$)

On another note, the reaction of $\mathbf{1}PF_6$ with Brønsted acid was explored envisioning that the hydrido moiety could undergo protonation rendering dihydrogen and eventually an accessible coordination vacant. As a matter of fact, $\mathbf{1}^+$ does react with Brønsted acids but with an unexpected outcome (Scheme 5). Indeed the reaction of $\mathbf{1}^+$ with HBF_4 (1 : 2 molar ratio) renders the hydrido iridium(III) derivative $[IrH(CH_2SiF_2CH_3)(HNP)_2(CN^tBu)_2][BF_4]$ ($\mathbf{7}BF_4$) [HNP = NH(4-tolyl)PPh_2] as a result of the formal addition of two hydrogen fluoride molecules to the κ^3C,P,P'-(SiNP–H) ligand along with the counterion exchange (Scheme 5). In addition, formally PF_5 and BF_3 should also result from the reaction, but unfortunately neither they nor any chemically related species could be identified in the course of the reaction.

The crystal structure of $\mathbf{7}BF_4$ was determined by means of single crystal X-ray diffraction measurements (Fig. 7). The metal centre exhibits an octahedral environment in which the newly formed ligands NH(4-tolyl)PPh_2 and $CH_2SiF_2CH_3$ are mutually *cis*, rendering an arrangement at the metal centre which is reminiscent of the κ^3C,P,P' coordination of the SiNP–H ligand of $\mathbf{1}^+$ [P(1)–Ir–P(2) 98.52(2)°, C(1)–Ir–P(2) 89.12(7)°, C(1)–Ir–P(1) 92.46(7)°]. The hydrido ligand lies *cis* to C1 and P1 and *trans* to P2 and the remaining *cis* coordination sites are occupied by the *tert*-butyl isocyanide ligands. Remarkably the N1–H1N group is involved in an intramolecular NH···F hydrogen bond to F1 [N1–H1N, 0.940(19); H1N···F1 2.11(2); N1···F1 3.001(3), N1–H1N–F1 158(3)°]. The crystal structure of $\mathbf{7}BF_4$ should be preserved in solution. Indeed two ^{31}P doublets are observed at 11.4 and 3.1 ppm with a coupling constant $^2J_{PP}$ of 20.5 Hz pointing at a *cis* disposition of the two HNP ligands. The ^1H NMR spectrum shows two singlets at 1.25 and 1.21 ppm, assigned to the *tert*-butyl isocyanide ligands, and a doublet of doublets of triplets at −11.86 ppm for the hydrido ligand as a result of the scalar coupling of the IrH hydrogen to the *trans* phosphorus ($^2J_{HP}$ = 152.9 Hz), the *cis* phosphorus ($^2J_{HP}$ = 17.4 Hz), and fluorine ($^4J_{HF}$ = 2.2 Hz). As for the $CH_2SiF_2CH_3$ moiety, two ^{19}F signals at −127.5 and −129.0 ppm ($^2J_{FF}$ = 20.6 Hz), and two ^1H multiplets at 0.01 and −0.42 ppm

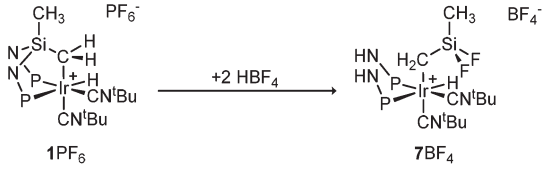

Scheme 5 Reaction of $[IrH\{\kappa^3C,P,P'\text{-(SiNP–H)}\}(CN^tBu)_2][PF_6]$ with HBF_4.

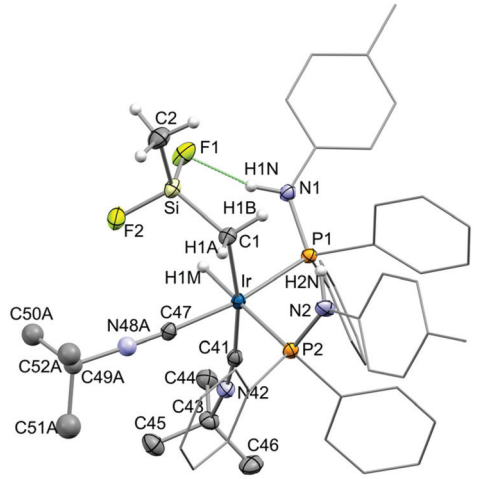

Fig. 7 ORTEP plot of $[IrH(CH_2SiF_2Me)(HNP)_2(CN^tBu)_2]^+$ ($\mathbf{7}^+$). For clarity, most hydrogen are omitted and the tolyl and phenyl rings are represented in a wireframe style. Selected bond lengths (Å) and angles (°) are given in ESI.†

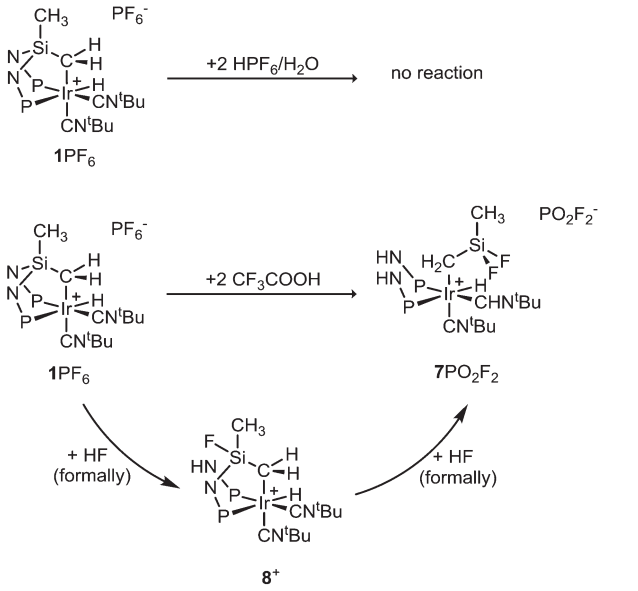

Scheme 6 Reaction of $[IrH\{\kappa^3C,P,P'\text{-}(SiNP-H)\}(CN^tBu)_2][PF_6]$ with HPF_6 or CF_3COOH.

for the $IrCH_2Si$ hydrogen atoms are observed (*cf.* Experimental section), which is indicative of two non-equivalent fluorine atoms and two non-equivalent hydrogen atoms, respectively. Also, while the $^{19}F\{^1H\}$ signal at −129.0 ppm is a doublet, the $^{19}F\{^1H\}$ signal at −127.5 ppm is a doublet of doublets due to the above mentioned fluorine–fluorine coupling and to a fluorine–phosphorus coupling ($^4J_{FP}$ = 2.7 Hz, *vide infra* for this assignment).

Remarkably the NH···F hydrogen bond observed in the solid state is maintained in solution. For the sake of clarity, the numbering scheme of the crystal structure given in Fig. 7 will be used in the following discussion of the NMR data. While a ^1H doublet ($^2J_{HP}$ = 15.9 ppm) at 4.21 ppm is observed for the N2–H2N moiety, a ^1H doublet of doublets at 5.33 ppm is observed for the N1–H1N group as a consequence of the scalar coupling of hydrogen to the phosphorus atom P1 ($^2J_{HP}$ = 15.9 Hz) and to the fluorine atom F1 (J_{HF} = 3.9 Hz). As a confirmation of the NH···F hydrogen bond and the consequent hampered rotation around the Ir–CH_2Si bond, NOE cross peaks are observed in the ^1H–^1H NOESY spectrum between H1B (−0.42 ppm) and H1N (5.35 ppm) and between H2N (4.21 ppm) and both H1A (0.01 ppm) and H1B (−0.42 ppm). Finally for the sake of confirmation, selected NMR data were calculated by DFT methods (mPW1PW91/def2TZVP) confirming the proposed assignment.‖

Aiming at investigating the influence of the acid – more specifically of its conjugated base – on the outcome of the reaction, $\mathbf{1}PF_6$ was treated with different Brønsted acids, namely HPF_6 in water (54% w/w) and CF_3COOH. Surprisingly no reaction between $\mathbf{1}PF_6$ and HPF_6 was observed even after 48 h at room temperature. On the other hand, the reaction of $\mathbf{1}PF_6$ with CF_3COOH is slower than that with HBF_4 and completeness is reached after 4 days and in the presence of a moderate excess of CF_3COOH (1 : 4) at room temperature, rendering $\mathbf{7}^+$ and the anion $PO_2F_2^-$. Notably when the reaction was monitored by $^{31}P\{^1H\}$ NMR spectroscopy, the anion PF_6^- is quantitatively converted into $PO_2F_2^-$ (δ_F = −84.1, δ_P = −19.5, $^1J_{PF}$ = 957 Hz) after 24 h. As a confirmation, the reaction of NBu_4PF_6 with CF_3COOH (1 : 4 molar ratio, in CD_2Cl_2) has a similar outcome cleanly affording $PO_2F_2^-$. On these grounds, reasonably the formation of $PO_2F_2^-$ should not be metal-assisted and might follow a route similar to the chlorination of carboxylic acids with PCl_5 and $POCl_3$.[8]

When the reaction of $\mathbf{1}^+$ with CF_3COOH was monitored by ^1H, ^{19}F and ^{31}P NMR spectroscopy, $[IrH\{\kappa^2C,P\text{-}CH_2SiMeFN(4\text{-tolyl})PPh_2\}(HNP)(CN^tBu)_2]^+$ ($\mathbf{8}^+$) was detected as an intermediate as a result of the formal addition of one hydrogen fluoride molecule to one Si–N bond (Scheme 6). Fig. 8 shows selected areas of the ^1H, ^{19}F and ^{31}P NMR spectra with the proposed assignment.**

‖ The calculated heteronuclear spin–spin constants J_{XY} are negligible in all the cases except for F2 and P2 (6.5 Hz, calc.), thus the observed fluorine-phosphorus coupling is the consequence of the conformation adopted by the F–Si–C–Ir–P fragment rather than of the NH···F hydrogen bond. On the other hand, when it comes to the NH···F hydrogen bond, the calculated heteronuclear spin–spin constants are negligible in all the cases except for H1N and F1 (23.2 Hz, calc.), nicely matching the proposed assignment.

** The $^{31}P\{^1H\}$ doublets at 43.0 and 11.9 ppm ($^2J_{PP}$ = 19.0 Hz) of $\mathbf{8}^+$ are indicative of two mutually *cis* phosphorus atoms. The ^{19}F doublet of quartets of doublets at −125.8 ppm results from the scalar coupling of the fluorine atom to the $SiCH_3$ moiety ($^3J_{HF}$ = 6.4 Hz) and the $SiCH_2$ non-equivalent hydrogen atoms ($^3J_{HF}$ = 16.4 Hz, 2.0 Hz). Accordingly, the ^1H doublet at 0.22 ppm ($^3J_{HF}$ = 6.4 Hz) was assigned to the $SiCH_3$ group (δ_C = −1.3 ppm, doublet, $^2J_{CF}$ = 6.7 Hz) and the ^1H multiplets at 0.20 and −0.24 ppm were assigned to the two non-equivalent $SiCH_2$ hydrogen

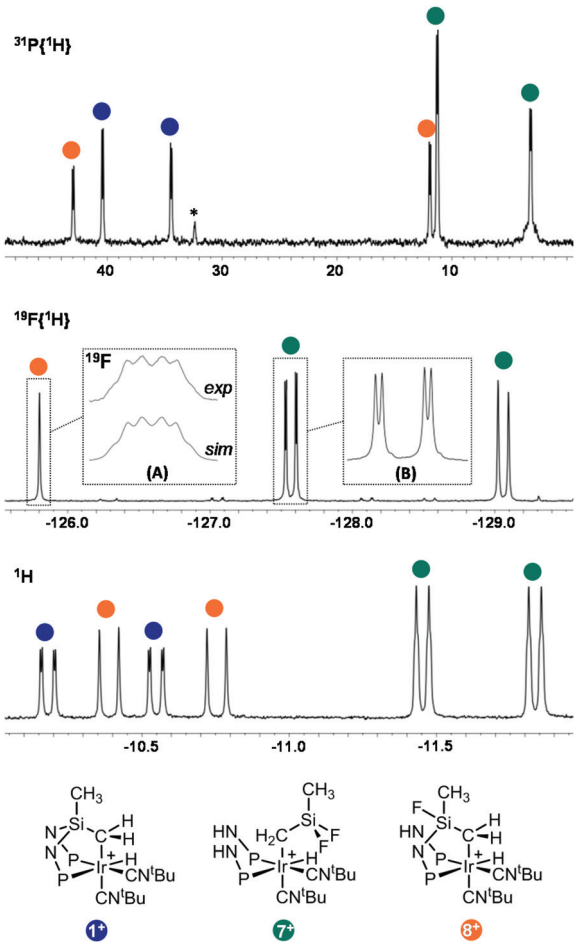

Fig. 8 Selected areas of the ^{1}H, ^{19}F, $^{19}F\{^{1}H\}$ and $^{31}P\{^{1}H\}$ NMR spectra of the mixture resulting from the reaction of $\mathbf{1}PF_6$ with CF_3COOH in CD_2Cl_2 after 24 h with the proposed assignment. Inset A shows the experimental and simulated ^{19}F signal at −125.8 ppm of $\mathbf{8}^+$. Inset B shows the expanded view of the $^{19}F\{^{1}H\}$ signal at −127.5 ppm of $\mathbf{7}^+$. * unassigned.

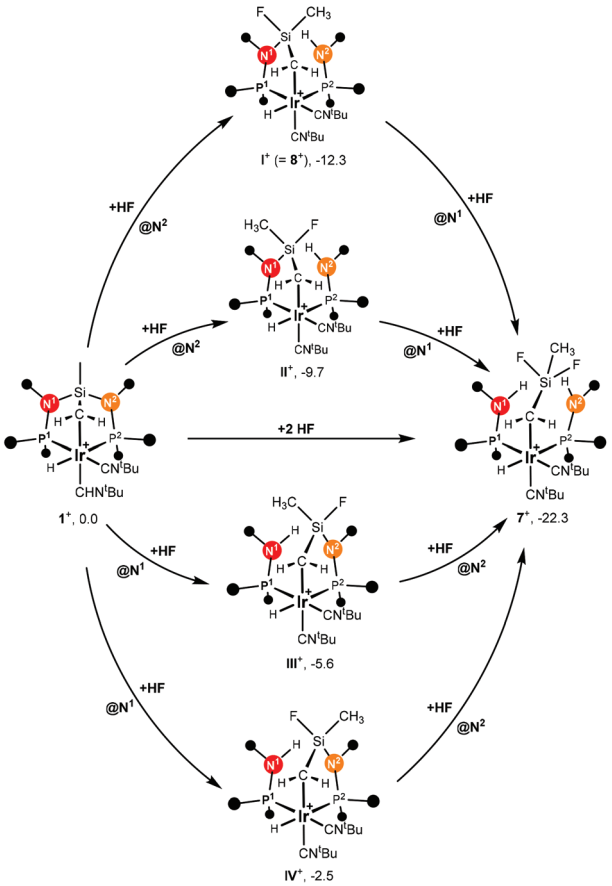

Fig. 9 Sequential addition of HF to $\mathbf{1}^+$ showing the possible intermediates and their relative Gibbs free energies (M06/def2tzvp//B3PW91-GD3BJ/def2svp, 298 K, 1 atm).

In view of the $^{31}P\{^{1}H\}$ and ^{1}H NMR spectra, the formal addition of hydrogen fluoride to $\mathbf{1}^+$ affording $\mathbf{8}^+$ is regiospecific since four products ($\mathbf{I}^+$–$\mathbf{IV}^+$, Fig. 9) might form depending on which nitrogen atom undergoes protonation (N^1 or N^2) and on the orientation of the formal addition of the fluoride ion to silicon (syn or anti with respect to the protonated nitrogen atom).

In order to shed light on the above mentioned regiospecificity, a thorough examination of the calculated structure of $\mathbf{1}^+$ suggested that the steric hindrances at each nitrogen atoms are similar. Further, the NBO charges of the nitrogen atoms are virtually identical (−1.171, −1.185 a.u.), suggesting that no preferential attack of H^+ to one of the two nitrogen atoms should be expected as a consequence of the atomic charges at the reacting sites. On these grounds, the observed selectivity in the formation of $\mathbf{8}^+$ should rely on the thermodynamic stability of the intermediate itself. With this in mind, the proton affinities (PA) of $\mathbf{1}^+$ were calculated along with the relative Gibbs free energy for the sequential addition of hydrogen fluoride to the two Si–N bonds $\mathbf{1}^+$, namely Si–N1 and Si–N2 (Fig. 9). In agreement with the proposed structure of $\mathbf{8}^+$, the most stable protonated species $\mathbf{1}H^{2+}$ is that resulting from the protonation of N2, that is the nitrogen atom bonded to the phosphorus *trans* to the hydrido moiety (PA = 143.2, N2; 139.4 kcal mol^{-1}, N1, Fig. 9). Accordingly, the most stable intermediate $\mathbf{I}^+$ results from the formal addition of hydrogen fluoride to the bond Si–N2 of $\mathbf{1}^+$ with an anti orientation of the attack of fluoride to silicon $\mathbf{1}^+$.

Conclusions

tert-Butyl isocyanide triggers the oxidative addition of the $SiCH_2$–H bond to iridium(I) in $[Ir(SiNP)(cod)][PF_6]$ yielding the iridium(III) hydrido derivative $[IrH\{\kappa^3C,P,P'\text{-}(SiNP\text{–}H)\}(CN^tBu)_2][PF_6]$ ($\mathbf{1}PF_6$). Reasonably as a consequence of the stable κ^3C,P,P' coordination of the SiNP–H ligand along with the substitutional inertness of the CN^tBu ligands, $\mathbf{1}^+$ as well as the related haloderivatives $[IrX\{\kappa^3C,P,P'\text{-}(SiNP\text{–}H)\}(CNtBu)_2]^+$

atoms. The ^{1}H signal of the hydrido ligand was observed at −10.8 ppm as a doublet of doublets ($^{2}J_{HP,\ trans}$ = 146.1 Hz, $^{2}J_{HP,\ cis}$ = 26.3 Hz).

(X = Cl, $\mathbf{4}^+$; Br, $\mathbf{5}^+$) and solvato complex $[Ir\{\kappa^3C,P,P'\text{-}(SiNP–H)\}(CH_3CN)(CN^tBu)_2]^{2+}$ ($\mathbf{6}^{2+}$) do not react with unsaturated molecules such as olefins or alkynes.

On the other hand, $\mathbf{1}^+$ does react with Brønsted acids such as HBF_4 and CF_3COOH undergoing the unexpected fragmentation of the SiNP backbone. Indeed the formal addition of two molecules of hydrogen fluoride to the Si–N bonds affords the iridium(III) derivative $[IrH(CH_2SiCH_3F_2)(HNP)_2(CN^tBu)_2]$ ($\mathbf{7}^+$) through the formation of the intermediate $[IrH\{\kappa^2C,P\text{-}CH_2SiMeFN(4\text{-tolyl})PPh_2\}(HNP)(CN^tBu)_2]^+$ ($\mathbf{8}^+$), observed as the result of the regiospecific formal addition of HF to one Si–N bond. Accordingly DFT calculation suggests that a sequential protonation of the Si–N–P moieties takes place followed by the formal addition of fluoride ion to silicon as well as that the observed regiospecificity relies on the thermodynamic stability of the observed intermediate.

Experimental

General section

All the operations were carried out using standard Schlenk tube techniques under an atmosphere of pre-purified argon or in a Braun glove-box under dinitrogen or argon. Organic solvents were dried by standard procedures and distilled under argon or obtained oxygen- and water-free from a Solvent Purification System (Innovative Technologies). The compounds $SiMe_2\{(N(4\text{-tolyl})(PPh_2)\}_2$ (SiNP)[6a] and $[Ir(SiNP)(cod)][PF_6]$[6b] were prepared according to the literature. NMR spectra were recorded with Bruker spectrometers (AV300 and AV400) and are referred to $SiMe_4$ (^1H, ^{13}C) and H_3PO_4 (^{31}P), $CFCl_3$ (^{19}F). The proposed ^1H, ^{13}C, and ^{31}P assignment relies on the combined analysis of 1D [^1H, $^1H\{^{31}P\}$, $^{13}C\{^1H\}$-apt, $^{31}P\{^1H\}$] and 2D NMR spectra (^1H–^1H COSY, ^1H–^1H NOESY, ^1H–^{13}C HSQC, ^1H–^{13}C HMBC, ^1H–^{31}P HMBC). In compounds containing two non-equivalent phosphorus atoms, namely P^1 and P^2, P^1 indicates the phosphorus atom *trans* to H ($\mathbf{1}^+$, $\mathbf{8}^+$), Cl ($\mathbf{4}^+$), Br ($\mathbf{5}^+$), or CH_3CN ($\mathbf{6}^{2+}$) and superscript labels "tol-P1/2" and "PhP1/2" are used for hydrogen and carbon atoms belonging to the tolyl and phenyl groups attached/linked to the phosphorus atom P1/2. C, H, and N analyses were carried out on a PerkinElmer 2400 CHNS/O analyzer.

Synthesis of $[IrH\{\kappa^3C,P,P'\text{-}(SiNP–H)\}(CN^tBu)_2][PF_6]$ ($\mathbf{1PF_6}$)

Method 1. A dichloromethane solution (15 mL) of $[Ir(SiNP)(cod)][PF_6]$ (199.80 mg, 0.184 mmol, 1084.15 g mol^{-1}) was added with CN^tBu (53.5 μL, 0.473 mmol, 83.13 g mol^{-1}, 0.735 g mL^{-1}). The yellow resulting solution was stirred for 24 h, partially evaporated up to 1 mL and added with hexane (5 mL), affording a pale yellow solid which was filtered off and washed with tetrahydrofuran/hexane (1 : 1, 5 mL), dried *in vacuo* and finally identified as $[IrH\{\kappa^3C,P,P'\text{-}(SiNP–H)\}(CN^tBu)_2][PF_6]$ ($\mathbf{1PF_6}$, 149 mg, 0.130 mmol, 71% yield).

Method 2. A dichloromethane solution (12 mL) of $[Ir(SiNP)(cod)(CN^tBu)][PF_6]$ ($\mathbf{2PF_6}$, *vide infra*, 619 mg, 0.530 mmol, 1167.29 g mol^{-1}) was added with CN^tBu (60.0 μL, 0.530 mmol, 83.13 g mol^{-1}, 0.735 g mL^{-1}) at 313 K. The resulting yellow solution was stirred for 14 h, partially evaporated and added with diethyl ether/hexane (1 : 1, 20 mL), affording a pale yellow solid which was filtered off and washed with tetrahydrofuran/hexane (1 : 1, 5 mL), dried *in vacuo* and finally identified as $[IrH\{\kappa^3C,P,P'\text{-}(SiNP–H)\}(CN^tBu)_2][PF_6]$ ($\mathbf{1PF_6}$, 464 mg, 0.406 mmol, 77% yield). Found: C, 52.99; H, 5.07; N, 4.85. Calcd for $C_{50}H_{58}F_6IrN_4P_3Si$ (1142.24): C, 52.57; H, 5.12; N, 4.91. ^1H NMR (CD_2Cl_2 298 K): δ_H 7.68–7.56 (6H tot; 4H, *o*-P^1Ph, 2H, *m*-P^1Ph), 7.55–7.43 (4H tot; 2H, *m*-P^2Ph, 2H, *p*-P^1Ph), 7.44–7.32 (6H tot; 2H, *p*-P^2Ph, 2H, *o*-P^2Ph, 2H, *m*-P^1Ph), 7.00 (d, 2H, $^3J_{HH}$ = 8.3 Hz, $C^3H^{tol\text{-}P2}$), 6.92 (td, 2H, $^3J_{HH}$ = 7.9 Hz, $^4J_{HP}$ = 2.3 Hz, *m*-P^2Ph), 6.76 (d, 2H, $^3J_{HH}$ = 8.3 Hz, $C^2H^{tol\text{-}P2}$), 6.74 (d, 2H, $^3J_{HH}$ = 8.3 Hz, $C^3H^{tol\text{-}P1}$), 6.61 (ddd, 2H, $^3J_{HP}$ = 11.5 Hz, $^3J_{HH}$ = 8.1 Hz, $^5J_{HP}$ = 1.1 Hz, *o*-P^2Ph), 6.24 (d, 2H, $^3J_{HH}$ = 8.3 Hz, $C^2H^{tol\text{-}P1}$), 2.29 (s, 3H, $CH_3^{tol\text{-}P1}$), 2.15 (s, 3H, $CH_3^{tol\text{-}P2}$), 1.37 (s, 9H, CH_3^{tBu}), 1.20 (s, 9H, CH_3^{tBu}), 0.67 (dddd, 1H, $^3J_{HP}$ = 15.0 Hz, $^2J_{HH}$ = 12.6 Hz, $^3J_{HH}$ = 2.6 Hz, $^3J_{HP}$ = 1.2 Hz, $SiCH^aH^bIr$), 0.46 (ddd, 1H, $^2J_{HH}$ = 12.6 Hz, $^3J_{HP}$ = 9.0 Hz, $^3J_{HP}$ = 1.2 Hz, $SiCH^aH^bIr$), −0.21 (s, 3H, $SiCH_3$,), −10.58 (ddd, 1H, $^2J_{HP\ trans}$ = 149.6 Hz, $^2J_{HP\ cis}$ = 17.9 Hz, $^3J_{HH}$ = 2.6 Hz, IrH). $^{13}C\{^1H\}$ NMR (CD_2Cl_2, 298 K): δ_C 140.2 (dd, $^1J_{CP}$ = 45.0 Hz, $^3J_{CP}$ = 1.9 Hz, $C^{1,\ PhP}$), 139.0 (d, $^2J_{CP}$ = 10.1 Hz, $C^{1,\ tol\text{-}P2}$), 138.5 (d, $^2J_{CP}$ = 9.6 Hz, $C^{1,\ tol\text{-}P1}$), 136.0 (d, $^5J_{CP}$ = 1.6 Hz, $C^{4,\ tol\text{-}P1}$), 135.5 ($C^{4,\ tol\text{-}P2}$), 135.4 (d, $^2J_{CP}$ = 13.8 Hz, $C^{2,\ PhP2}$), 134.64 (d, $^1J_{CP}$ = 60.2 Hz, $C^{1,\ PhP}$), 134.60 (d, $^2J_{CP}$ = 12.0 Hz, $^4J_{CP}$ = 1.2 Hz $C^{2,\ PhP1}$), 133.90 (dd, $^1J_{CP}$ = 63.4 Hz, $^3J_{CP}$ = 4.5 Hz, $C^{1,\ PhP}$), 131.8 (d, $^2J_{CP}$ = 10.9 Hz, $C^{2,\ PhP1}$), 131.7 (d, $^4J_{CP}$ = 2.2 Hz, $C^{4,\ PhP2}$), 131.5 (d, $^4J_{CP}$ = 2.0 Hz, $C^{4,\ PhP1}$), 131.1 (d, $^4J_{CP}$ = 2.4 Hz, $C^{4,\ PhP2}$), 130.5 (d, $^2J_{CP}$ = 10.2 Hz, $C^{2,\ PhP2}$), 130.3 (d, $^4J_{CP}$ = 2.0 Hz, $C^{4,\ PhP1}$), 129.7 (d, $^4J_{CP}$ = 1.4 Hz, $C^{3,\ tol\text{-}P2}$), 129.64 (d, $^4J_{CP}$ = 0.7 Hz, $C^{3,\ tol\text{-}P1}$), 129.61 (d, $^4J_{CP}$ = 1.4 Hz, $C^{2,\ tol\text{-}P1}$), 129.1 (d, $^3J_{CP}$ = 1.4 Hz, $C^{2,\ tol\text{-}P2}$), 128.4 (d, $^3J_{CP}$ = 10.8 Hz, $C^{3,\ PhP2}$), 128.3 (d, $^3J_{CP}$ = 9.7 Hz, $C^{3,\ PhP1}$), 128.0 (d, $^3J_{CP}$ = 11.1 Hz, $C^{3,\ PhP2}$), 127.4 (d, $^3J_{CP}$ = 10.8 Hz, $C^{3,\ PhP1}$), 58.4 (C^{tBu2}), 58.2 (C^{tBu1}), 30.0 (CH_3^{tBu1}), 29.8 (CH_3^{tBu2}), 20.5 ($CH_3^{tol\text{-}P2}$), 20.4 ($CH_3^{tol\text{-}P1}$), −0.9 (t, $^3J_{CP}$ = 7.6 Hz, CH_3Si), −29.7 (dd, $^2J_{CP}$ = 3.7, 2.1 Hz, CH_2Si). $^{31}P\{^1H\}$ NMR (CD_2Cl_2, 298 K): δ_P 40.3 (d, $^2J_{PP}$ 20.4 Hz, $P^{1,\ SiNP}$), 34.4 (d, $^2J_{PP}$ 20.4 Hz, $P^{2,\ SiNP}$), −144.4 (hept, $^1J_{PF}$ = 710.2 Hz, PF_6^-).

Synthesis of $[Ir(SiNP)(cod)(CN^tBu)][PF_6]$ ($\mathbf{2PF_6}$)

A dichloromethane solution (10 mL) of $[Ir(SiNP)(cod)][PF_6]$ (178 mg, 0.164 mmol, 1084.15 g mol^{-1}) was added with CN^tBu (37.4 μL, 0.331 mmol, 83.13 g mol^{-1}, 0.735 g mL^{-1}) at 253 K. The yellow resulting solution was stirred for 30 minutes, partially evaporated and added with hexane (10 mL) affording a light yellow solid which was filtered off, dried *in vacuo* and finally identified as $[Ir(SiNP)(cod)(CN^tBu)][PF_6]$ ($\mathbf{2PF_6}$, 176 mg, 0.151 mmol, 92% yield). Found: C, 53.97; H, 5.31; N, 3.65. Calcd for $C_{53}H_{61}F_6IrN_3P_3Si$ (1167.29): C, 54.53; H, 5.27; N, 3.60. ^1H NMR (C_6D_6 298 K), *the labels "up" and "down" are used for the CH or CH_3 moieties pointing towards the CN^tBu ligand and apart from it*, *respectively*: δ_H 7.70–7.55 (8H, *o*-PPh), 7.43–7.24 (12H, *m*-PPh and *p*-PPh), 7.19 (d, 2H, $^3J_{HH}$ = 8.2 Hz, $C^2H^{tol\ down}$), 6.83 (d, 2H, $^3J_{HH}$ = 8.2 Hz, $C^3H^{tol\ down}$), 6.64 (d, 2H, $^3J_{HH}$ = 8.2 Hz, $C^3H^{tol\ up}$), 6.24 (d, 2H, $^3J_{HH}$ = 8.2 Hz, C^2H^{tol}

up}), 3.47 (br, 4H, $C^{sp2}H^{cod}$), 2.03 (s, 6H, $CH_3{}^{tol}$), 1.97 (s, 9H, $CH_3{}^{tBu}$), 1.76 (br, 8H, $C^{sp3}H^{cod}$), 0.56 (s, 3H, $SiCH_3{}^{up}$), −0.21 (s, 3H, $SiCH_3{}^{down}$). $^{13}C\{^1H\}$ NMR (C_6D_6, 298 K): δ_C 139.6 ($C^{4,\ tol}$), 136.7 ($C^{1,\ tol}$), 135.6 ($C^{2,\ PhP}$), 132.6 ($C^{2,\ PhP}$), 132.0–131.9 ($C^{2,\ tol\ up}$ and $C^{2,\ tol\ down}$), 131.8 ($C^{3,\ PhP}$), 130.5 ($C^{4,\ PhP}$), 129.6 ($C^{3,\ tol\ down}$), 129.1 ($C^{3,\ tol\ up}$), 127.6 ($C^{3,\ PhP}$), 78.4 ($C^{sp2,\ cod}$), 59.9 (C^{tBu}), 32.6 ($C^{sp3,\ cod}$), 30.4 ($CH_3{}^{tBu}$) 20.5 ($CH_3{}^{tol}$), 3.4 (t, $^3J_{CP}$ = 2.2 Hz, CH_3Si^{down}), 2.1 (CH_3Si^{up}). $^{31}P\{^1H\}$ NMR (C_6D_6, 298 K): δ_P 41.3 (s, P^{SiNP}), −142.5 (hept, $^1J_{PF}$ = 708.8 Hz, PF_6^-).

Synthesis of [IrCl{κ³*C*,*P*,*P*′-(SiNP–H)}(CN^{t}Bu)$_2$][PF$_6$] (4PF$_6$)

A dichloromethane solution (8 mL) of [IrH{κ³*C*,*P*,*P*′-(SiNP–H)}(CN^{t}Bu)$_2$][PF$_6$] (**1**PF$_6$, 87.3 mg, 0.0764 mmol, 1142.24 g mol^{-1}) was added with *N*-chlorosuccinimide (10.1 mg, 0.0756 mmol, 133.53 g mol^{-1}). The resulting colourless solution was stirred for 32 h, partially evaporated and added with hexane (5 mL), affording a colourless solid which was filtered off and washed with diethyl ether (3 × 5 mL), dried *in vacuo* and finally identified as [IrCl{κ³*C*,*P*,*P*′-(SiNP–H)}(CN^{t}Bu)$_2$][PF$_6$] (**4**PF$_6$, 81.5 mg, 0.0693 mmol, 92% yield). Found: C, 51.65; H, 4.78; N, 4.70. Calcd for $C_{50}H_{57}ClF_6IrN_4P_3Si$ (1176.68): C, 51.04; H, 4.88; N, 4.76. ^1H NMR (CD_2Cl_2 298 K): δ_H 7.62–7.47 (10H tot: 4H, *o*-PPh, 4H, *m*-P^{2}Ph, 2H, *p*-P^{2}Ph), 7.45 (m, 2H, *m*-P^{1}Ph), 7.43–7.31 (4H tot: 2H *o*-P^{1}Ph, 2H *p*-P^{2}Ph), 7.11 (td, 2H, $^3J_{HH}$ = 7.9 Hz, $^3J_{HP}$ = 3.0 Hz, *m*-P^{2}Ph), 6.92 (d, 2H, $^3J_{HH}$ = 8.2 Hz, $C^3H^{tol\text{-}P2}$), 6.86 (ddd, 2H, $^3J_{HP}$ = 12.5 Hz, $^3J_{HH}$ = 8.2 Hz, $^3J_{HP}$ = 1.0 Hz, *o*-P^{2}Ph), 6.81 (d, 2H, $^3J_{HH}$ = 8.2 Hz, $C^3H^{tol\text{-}P1}$), 6.52 (d, 2H, $^3J_{HH}$ = 8.2 Hz, $C^2H^{tol\text{-}P2}$), 6.41 (d, 2H, $^3J_{HH}$ = 8.2 Hz, $C^2H^{tol\text{-}P1}$), 2.24 (s, 3H, $CH_3{}^{tol\text{-}P1}$), 2.18 (s, 3H, $CH_3{}^{tol\text{-}P2}$), 1.45 (s, 9H, $CH_3{}^{tBu2}$), 1.30 (dd, 1H, $^2J_{HH}$ = 13.1 Hz, $^3J_{HP}$ = 6.6 Hz, $SiCH_2Ir$), 1.25 (s, 9H, $CH_3{}^{tBu1}$), 1.21 (ddd, 1H, $^2J_{HH}$ = 13.1 Hz, $^3J_{HP}$ = 3.6 Hz, $^3J_{HP}$ = 1.3 Hz, $SiCH_2Ir$), 0.15 (s, 3H, $SiCH_3$). $^{13}C\{^1H\}$ NMR (CD_2Cl_2, 298 K): δ_C 138.3 (d, $^1J_{CP}$ = 67.5 Hz, $C^{1,\ PPh}$), 137.6 (d, $^2J_{CP}$ = 9.6 Hz, $C^{1,\ tol\text{-}P1}$), 137.2 ($C^{1,\ tol\text{-}P2}$), 136.5 (d, $^5J_{CP}$ = 1.9 Hz, $C^{4,\ tol\text{-}P2}$), 135.8 (d, $^5J_{CP}$ = 1.5 Hz, $C^{4,\ tol\text{-}P1}$), 134.3 (d, $^2J_{CP}$ = 10.0 Hz, $C^{2,\ PhP1}$), 134.2 (d, $^2J_{CP}$ = 10.6 Hz, $C^{2,\ PhP2}$), 133.2 (d, $^2J_{CP}$ = 10.8 Hz, $C^{2,\ PhP2}$), 132.4 (d, $^4J_{CP}$ = 2.8 Hz, $C^{4,\ PhP2}$), 132.04 (d, $^4J_{CP}$ = 2.9 Hz, $C^{4,\ PhP1}$), 131.99 (d, $^4J_{CP}$ = 2.8 Hz, $C^{4,\ PhP2}$), 131.4 (d, $^4J_{CP}$ = 2.7 Hz, $C^{4,\ PhP1}$), 131.1 (d, $^2J_{CP}$ = 10.2 Hz, $C^{2,\ PhP1}$), 129.8 (d, $^5J_{CP}$ = 1.7 Hz, $C^{3,\ tol\text{-}P2}$), 129.5 ($C^{3,\ tol\text{-}P1}$), 129.2 (d, $^4J_{CP}$ = 3.4 Hz, $C^{2,\ tol\text{-}P2}$), 128.8 (d, $^3J_{CP}$ = 11.5 Hz, $C^{3,\ PhP1}$), 128.6 (dd, $^3J_{CP}$ = 6.6 Hz, $^5J_{CP}$ = 3.2 Hz, $C^{2,\ tol\text{-}P1}$), 128.5 (d, $^3J_{CP}$ = 11.3 Hz, $C^{3,\ PhP1}$), 127.9 (d, $^3J_{CP}$ = 11.7 Hz, $C^{3,\ PhP2}$), 127.2 (d, $^3J_{CP}$ = 11.3 Hz, $C^{3,\ PhP1}$), 59.3 (C^{tBu2}), 59.0 (C^{tBu1}), 29.8 ($CH_3{}^{tBu1}$), 29.7 ($CH_3{}^{tBu2}$), 20.5 ($CH_3{}^{tol\text{-}P2}$), 20.3 ($CH_3{}^{tol\text{-}P1}$), −1.2 (t, $^3J_{CP}$ = 7.0 Hz, CH_3Si), −16.2 (CH_2Si). $^{31}P\{^1H\}$ NMR (CD_2Cl_2, 298 K): δ_P 28.6 (d, $^2J_{PP}$ = 18.2 Hz, $SiNP^1$), 26.3 (d, $^2J_{PP}$ = 18.2 Hz, $SiNP^2$), −144.4 (hept, $^1J_{PF}$ = 710.2 Hz, PF_6^-).

Synthesis of [IrBr{κ³*C*,*P*,*P*′-(SiNP–H)}(CN^{t}Bu)$_2$][PF$_6$] (5PF$_6$)

A dichloromethane solution (8 mL) of [IrH{κ³*C*,*P*,*P*′-(SiNP–H)}(CN^{t}Bu)$_2$][PF$_6$] (**1**PF$_6$, 175 mg, 0.153 mmol, 1142.24 g mol^{-1}) was added with *N*-bromosuccinimide (27.3 mg, 0.153 mmol, 177.98 g mol^{-1}). The resulting colourless solution was stirred for 30 min, partially evaporated and added with hexane (5 mL), affording a colorless solid which was filtered off and washed with diethyl ether (3 × 5 mL), dried *in vacuo* and finally identified as [IrBr{κ³*C*,*P*,*P*′-(SiNP–H)}(CN^{t}Bu)$_2$][PF$_6$] (**5**PF$_6$, 147 mg, 0.120 mmol, 79% yield). Found: C, 49.27; H, 4.72; N, 4.39. Calcd for $C_{50}H_{57}BrF_6IrN_4P_3Si$ (1221.13): C, 49.18; H, 4.70; H, 4.59. ^1H NMR (CD_2Cl_2 298 K): δ_H 7.66–7.41 (12H tot: 4H *o*-PPh, 4H *m*-PPh, 4H *p*-PPh), 7.37–7.28 (4H tot: 2H *o*-P^{1}Ph, 2H *m*-P^{1}Ph), 7.15 (td, 2H, $^3J_{HH}$ = 7.9 Hz, $^4J_{HP}$ = 3.0 Hz, *m*-P^{2}Ph), 6.94 (ddd, 2H, $^3J_{HP}$ = 12.3 Hz, $^3J_{HH}$ = 7.9 Hz, $^5J_{HP}$ = 1.1 Hz, *o*-P^{2}Ph), 6.91 (d, 2H, $^3J_{HH}$ = 8.2 Hz, $C^3H^{tol\text{-}P2}$), 6.83 (d, 2H, $^3J_{HH}$ = 8.2 Hz, $C^3H^{tol\text{-}P1}$), 6.50 (d, 2H, $^3J_{HH}$ = 8.2 Hz, $C^2H^{tol\text{-}P2}$), 6.43 (d, 2H, $^3J_{HH}$ = 8.2 Hz, $C^2H^{tol\text{-}P1}$), 2.24 (s, 3H, $CH_3{}^{tol\text{-}P2}$), 2.19 (s, 3H, $CH_3{}^{tol\text{-}P1}$), 1.44 (s, 9H, $CH_3{}^{tBu1}$), 1.37 (ddd, 1H, $^2J_{HH}$ = 13.2 Hz, $^3J_{HP}$ = 3.3 Hz, $^3J_{HP}$ = 1.3 Hz, $SiCH_2Ir$), 1.25 (s, 9H, $CH_3{}^{tBu2}$), 1.24 (dd, 1H, $^2J_{HH}$ = 13.2 Hz, $^3J_{HP}$ = 8.6 Hz, $SiCH_2Ir$), 0.17 (s, 3H, $SiCH_3$). $^{13}C\{^1H\}$ NMR (CD_2Cl_2, 298 K): δ_C 137.8 (dd, $^1J_{CP}$ = 65.3 Hz, $^3J_{CP}$ = 2.7 Hz, $C^{1,\ PhP}$), 137.7 (d, $^2J_{CP}$ = 9.1 Hz, $C^{1,\ tol\text{-}P1}$), 137.1 (d, $^2J_{CP}$ = 9.0 Hz, $C^{1,\ tol\text{-}P2}$), 136.4 (d, $^5J_{CP}$ = 2.0 Hz, $C^{4,\ tol\text{-}P2}$), 135.8 (d, $^5J_{CP}$ = 1.6 Hz, $C^{4,\ tol\text{-}P1}$), 134.1 (d, $^2J_{CP}$ = 10.1 Hz, $C^{2,\ PhP2}$), 134.0 (d, $^2J_{CP}$ = 10.0 Hz, $C^{2,\ PhP1}$), 133.4 (d, $^2J_{CP}$ = 10.8 Hz, $C^{2,\ PhP1}$), 132.5 (d, $^4J_{CP}$ = 2.7 Hz, $C^{4,\ PhP2}$), 132.1 (d, $^4J_{CP}$ = 2.8 Hz, $C^{4,\ PhP1}$), 132.0 (d, $^4J_{CP}$ = 2.5 Hz, $C^{4,\ PhP2}$), 131.5 (dd, $^1J_{CP}$ = 62.7 Hz, $^3J_{CP}$ = 1.6 Hz, $C^{1,\ PhP}$), 131.4 (d, $^4J_{CP}$ = 2.8 Hz, $C^{4,\ PhP1}$), 131.3 (d, $^3J_{CP}$ = 10.1 Hz, $C^{2,\ PhP2}$), 130.3 (dd, $^1J_{CP}$ = 57.1 Hz, $^3J_{CP}$ = 1.4 Hz, $C^{1,\ PhP}$), 129.7 (d, $^5J_{CP}$ = 1.6 Hz, $C^{3,\ tol\text{-}P2}$), 129.5 (d, $^5J_{CP}$ = 1.2 Hz, $C^{3,\ tol\text{-}P1}$), 129.0 (d, $^4J_{CP}$ = 3.5 Hz, $C^{2,\ tol\text{-}P2}$), 128.8 (d, $^2J_{CP}$ = 11.3 Hz, $C^{3,\ PhP2}$), 128.6 (d, $^4J_{CP}$ = 3.3 Hz, $C^{2,\ tol\text{-}P1}$), 128.40 (d, $^3J_{CP}$ = 10.8 Hz, $C^{3,\ PhP1}$), 128.37 (dd, $^1J_{CP}$ = 66.5 Hz, $^3J_{CP}$ = 1.2 Hz, $C^{1,\ PhP}$), 128.1 (d, $^3J_{CP}$ = 11.6 Hz, $C^{3,\ PhP2}$), 127.2 (d, $^3J_{CP}$ = 11.2 Hz, $C^{3,\ PhP1}$), 59.3 (C^{tBu2}), 58.9 (C^{tBu1}), 29.8 ($CH_3{}^{tBu1}$), 29.6 ($CH_3{}^{tBu2}$), 20.4 ($CH_3{}^{tol\text{-}P2}$), 20.4 ($CH_3{}^{tol\text{-}P1}$), −1.1 (t, $^3J_{CP}$ = 7.1 Hz, CH_3Si), −18.9 (d, $^2J_{CP}$ = 3.8 Hz, CH_2Si). $^{31}P\{^1H\}$ NMR (CD_2Cl_2, 298 K): δ_P 25.7 (d, $^2J_{PP}$ = 17.4 Hz, $P^{1\ SiNP}$), 25.1 (d, $^2J_{PP}$ = 17.4 Hz, $P^{2\ SiNP}$), −144.4 (hept, $^1J_{PF}$ = 710.2 Hz, PF_6^-).

Synthesis of [Ir{κ³*C*,*P*,*P*′-(SiNP–H)}(CH$_3$CN)(CN^{t}Bu)$_2$][PF$_6$]$_2$ (6[PF$_6$]$_2$)

An acetonitrile solution (10 mL) of [IrBr{κ³*C*,*P*,*P*′-(SiNP–H)}(CN^{t}Bu)$_2$][PF$_6$] (**5**PF$_6$, 233 mg, 0.191 mmol, 1221.13 g mol^{-1}) was added with $AgPF_6$ (53.2 mg, 0.210 mmol, 252.83 g mol^{-1}). The resulting colorless suspension was stirred for 12 h and filtered. The resulting solution was partially evaporated and added with diethyl ether (5 mL), affording a colourless solid which was filtered and washed with diethyl ether (3 × 5 mL), dried *in vacuo* and finally identified as [Ir(CH$_3$CN){κ³*C*,*P*,*P*′-(SiNP–H)}(CN^{t}Bu)$_2$][PF$_6$]$_2$ (**6**[PF$_6$]$_2$, 179 mg, 0.0135 mmol, 71% yield). Found: C, 46.81; H, 4.69; N, 5.32. Calcd for: $C_{52}H_{60}F_{12}IrN_5P_4Si$ (1327.24): C, 47.06; H, 4.56; N, 5.28. ^1H NMR (CD_2Cl_2 298 K): δ_H 7.73–7.46 (12H tot: 4H *m*-PPh, 4H *p*-PPh, 4H *o*-PPh), 7.46–7.31 (4H tot: 2H *o*-P^{2}Ph, 2H *m*-P^{2}Ph), 7.18 (td, 2H, $^3J_{HH}$ = 7.8 Hz, $^3J_{HP}$ = 3.2 Hz, *m*-P^{1}Ph), 6.95 (m, 2H, *m*-P^{2}Ph), 6.90 (br d, 4H, $^3J_{HH}$ = 8.0 Hz, $C^3H^{tol\text{-}P1}$ and $C^3H^{tol\text{-}P2}$), 6.50 (d, 2H, $^3J_{HH}$ = 8.0 Hz $C^2H^{tol\text{-}P1}$), 6.41 (d, 2H, $^3J_{HH}$ = 8.0 Hz, $C^2H^{tol\text{-}P2}$), 2.23 (br s, 6H, $CH_3{}^{tol\text{-}P1}$ and $CH_3{}^{tol\text{-}P2}$), 2.09 (s, 3H, CH_3CN), 1.48 (s, 9H, $CH_3{}^{tBu1}$), 1.44 (dd, 1H, $^2J_{HH}$ = 13.0 Hz, $^3J_{HP}$ = 7.5 Hz, $SiCH_2Ir$), 1.30 (dd, 1H, $^2J_{HH}$ = 13.0 Hz, $^3J_{HP}$ = 2.7

Hz, $SiCH_2Ir$), 1.29 (s, 9H, $CH_3{}^{tBu2}$), 0.34 (s, 3H, $SiCH_3$). $^{13}C\{^1H\}$ NMR (CD_2Cl_2, 298 K): δ_C 137.0 (d, $^5J_{CP}$ = 2.1 Hz, $C^{4,\ tol\text{-}P2}$), 136.7 (d, $^2J_{CP}$ = 8.7 Hz, $C^{1,\ tol1}$ or $C^{1,\ tol2}$), 136.5 (d, $^5J_{CP}$ = 1.5 Hz, $C^{4,\ tol\text{-}P1}$), 135.81 (d, $^2J_{CP}$ = 8.0 Hz, $C^{1,\ tol1}$ or $C^{1,\ tol2}$), 135.79 (d, $^2J_{CP}$ = 70.6 Hz, $C^{2,\ PhP}$), 133.9 (d, $^2J_{CP}$ = 10.7 Hz, $C^{2,\ PhP2}$), 133.7 (d, $^2J_{CP}$ = 11.1 Hz, $C^{2,\ PhP1}$), 133.2 (d, $^4J_{CP}$ = 2.8 Hz, $C^{4,\ PhP2}$), 133.0 (d, $^4J_{CP}$ = 1.9 Hz, $C^{4,\ PhP1}$), 132.9 (d, $^4J_{CP}$ = 1.8 Hz, $C^{4,\ PhP2}$), 132.5 (d, $^4J_{CP}$ = 2.8 Hz, $C^{4,\ PhP1}$), 132.3 (d, $^3J_{CP}$ = 10.1 Hz, $C^{2,\ PhP2}$), 131.4 (d, $^3J_{CP}$ = 10.2 Hz, $C^{2,\ PhP1}$), 130.8 (d, $^1J_{CP}$ = 60.7 Hz, $C^{1,\ PhP}$), 130.0 (d, $^4J_{CP}$ = 1.5 Hz, $C^{3,\ tol\text{-}P2}$), 129.9 (d, $^4J_{CP}$ = 1.4 Hz, $C^{3,\ tol\text{-}P1}$), 129.4 (d, $^3J_{CP}$ = 11.7 Hz, $C^{2,\ PhP2}$), 129.4 (d, $^3J_{CP}$ = 11.2 Hz, $C^{2,\ PhP1}$), 129.1 (d, $^3J_{CP}$ = 11.7 Hz, $C^{3,\ PhP2}$), 128.9 (d, $^4J_{CP}$ = 3.7 Hz, $C^{2,\ tol\text{-}P2}$), 128.6 (d, $^3J_{CP}$ = 12.0 Hz, $C^{3,\ PhP1}$), 127.8 (d, $^4J_{CP}$ = 3.8 Hz, $C^{2,\ tol\text{-}P1}$), 127.7 (d, $^1J_{CP}$ = 62.0 Hz, $C^{1,\ PhP}$), 126.8 (d, $^1J_{CP}$ = 70.9 Hz, $C^{1,\ PhP}$), 121.9 (d, $^3J_{CP}$ = 18.6 Hz, $NCCH_3$), 61.1 (C^{tBu2}), 60.7 (C^{tBu1}), 29.4 ($CH_3{}^{tBu1}$), 29.3 ($CH_3{}^{tBu2}$), 20.4 ($CH_3{}^{tol1\ or\ tol2}$), 20.3 ($CH_3{}^{tol1\ or\ tol2}$), 2.6 (CH_3CN), −1.5 (t, $^3J_{CP}$ = 6.8 Hz, CH_3Si), −18.7 (t, $^2J_{CP}$ = 3.6 Hz, CH_2Si). $^{31}P\{^1H\}$ NMR (CD_2Cl_2, 298 K): δ_P 25.1 (d, $^2J_{PP}$ 19.4 Hz, $P^{1\ SiNP}$), 18.0 (d, $^2J_{PP}$ 19.4 Hz, $P^{2\ SiNP}$), −144.4 (hept, $^1J_{PF}$ = 710.2 Hz, PF_6^-).

Synthesis of $[IrH(CH_2SiF_2CH_3)(HNP)_2(CN^tBu)_2][BF_4]$ (7BF_4)

A dichloromethane solution (5 mL) of $[IrH(SiNP–H)(CN^tBu)_2][PF_6]$ (**1**PF_6, 116 mg, 0.102 mmol, 1142.24 g mol^{-1}) was added with $HBF_4{\cdot}Et_2O$ (27.8 μL, 0.203 mmol, 161.93 g mol^{-1}, 1.18 g mL^{-1}) at 193 K. The resulting colourless solution was stirred for 30 min, allowed to warm up at room temperature, partially evaporated and added with hexane (10 mL), affording a colourless solid which was filtered off and washed with diethyl ether/hexane (1 : 10) (12 mL), dried *in vacuo* and finally identified as $[IrH(CH_2SiF_2CH_3)(HNP)_2(CN^tBu)_2][BF_4]$ (7BF_4, 64.4 mg, 0.0573 mmol, 56% yield). Found: C, 53.29; H, 5.47; N, 5.09. Calcd for $C_{50}H_{60}BF_6IrN_4P_2Si$ (1124.09): C, 53.42; H, 5.38; N, 4.98. ^1H NMR (CD_2Cl_2 298 K): δ_H 7.74–7.62 (4H tot: 2H *p*-P^2Ph and 2H *o*-P^2Ph), 7.62–7.45 (12H tot: 2H *o*-P^1Ph, 2H *o*-P^2Ph, 4H *m*-P^1Ph, 2H *m*-P^2Ph and 2H *p*-P^1Ph,), 7.40 (td, 2H, $^3J_{HH}$ = 7.7 Hz, $^4J_{HP}$ = 2.8 Hz, *m*-P^2Ph), 7.31 (m, 2H, *o*-P^1Ph), 6.77 (d, 2H, $^3J_{HH}$ = 8.4 Hz, $C^3H^{tol\text{-}P1}$), 6.73 (d, $^3J_{HH}$ = 8.4 Hz, $C^3H^{tol\text{-}P2}$), 6.11 (d, 2H, $^3J_{HH}$ = 8.4 Hz, $C^2H^{tol\text{-}P1}$), 5.94 (d, 2H, $^3J_{HH}$ = 8.4 Hz, $C^2H^{tol\text{-}P2}$), 5.33 (dd, 1H, $^2J_{HP}$ = 15.9 Hz, $^1J_{HF}$ = 3.9 Hz, NH^{P1}), 4.21 (d, 1H, $^2J_{HP}$ = 15.9 Hz, NH^{P2}), 2.16 (s, 3H, $CH_3{}^{tol\text{-}P1}$), 2.15 (s, 3H, $CH_3{}^{tol\text{-}P2}$), 1.25 (s, 9H, $CH_3{}^{tBu1}$), 1.21 (s, 9H, $CH_3{}^{tBu2}$), 0.33 (t, 3H, $^3J_{HF}$ = 6.3 Hz, $SiCH_3$), 0.01 (ddddd, 1H, $^2J_{HH}$ = 13.4 Hz, $^3J_{HF}$ = 13.4 Hz, $^3J_{HP}$ = 10.5 Hz, $^3J_{HP}$ = 4.7 Hz, $^3J_{HF}$ = 2.4 Hz, $SiCH^aH^bIr$), −0.42 (ddddd, 1H, $^2J_{HH}$ = 13.4 Hz, $^3J_{HF}$ = 13.4 Hz, $^3J_{HP}$ = 11.6 Hz, $^3J_{HP}$ = 3.6 Hz, $^3J_{HF}$ = 3.5 Hz, $SiCH^aH^bIr$), −11.86 (ddt, 1H, $^2J_{HP\ trans}$ = 152.9 Hz, $^2J_{HP\ cis}$ = 17.4 Hz, $^4J_{HF}$ = 2.2 Hz, IrH). $^{13}C\{^1H\}$ NMR (CD_2Cl_2, 298 K): δ_C 138.9 (d, $^2J_{CP}$ = 9.0 Hz, $C^{1,\ tol\text{-}P2}$), 138.0 (d, $^2J_{CP}$ = 11.1 Hz, $C^{1,\ tol\text{-}P1}$), 132.2 (d, $^2J_{CP}$ = 10.2 Hz, $C^{2,\ PhP1}$), 131.9 (d, $^4J_{CP}$ = 2.3 Hz, $C^{4,\ PhP1}$), 131.73 (d, $^3J_{CP}$ = 10.6 Hz, $C^{2,\ PhP2}$), 131.67 (d, $^3J_{CP}$ = 11.0 Hz, $C^{2,\ PhP2}$), 131.5 (dd, $^3J_{CP}$ = 10.0, $^5J_{CP}$ = 2.8 Hz, $C^{2,\ PhP1}$), 130.8 ($C^{4,\ tol\text{-}P1}$ and $C^{4,\ tol\text{-}P2}$), 130.7 (d, $^3J_{CP}$ = 11.2 Hz, $C^{3,\ PhP1}$), 129.1 (d, $^3J_{CP}$ = 11.2 Hz, $C^{3,\ tol\text{-}P1}$), 129.0 (d, $^4J_{CP}$ = 7.6 Hz, $C^{3,\ tol\text{-}P2}$), 128.9 (d, $^4J_{CP}$ = 1.6 Hz, $C^{4,\ PhP2}$), 128.6 (d, $^3J_{CP}$ = 11.2 Hz, $C^{3,\ PhP2}$), 118.4 (d, $^3J_{CP}$ = 5.7 Hz, $C^{2,\ tol\text{-}P1}$), 117.9 (d, $^3J_{CP}$ = 5.1 Hz, $C^{2,\ tol\text{-}P1}$), 58.9 (C^{tBu2}), 58.8 (C^{tBu1}), 29.7 ($CH_3{}^{tBu1}$), 29.4 ($CH_3{}^{tBu2}$), 20.0 ($CH_3{}^{tol\text{-}P1}$), 20.0 ($CH_3{}^{tol\text{-}P2}$), −3.6 (t, $^2J_{CF}$ = 19.3 Hz, CH_3Si), −34.9 (CH_2Si). $^{19}F\{^1H\}$ NMR (CD_2Cl_2, 298 K): δ_F −127.5 (dd, 1F, $^2J_{FF}$ = 20.6 Hz, $^4J_{FP}$ = 2.7 Hz, SiF^aF^b), −129.0 (d, 1F, $^2J_{FF}$ = 20.6 Hz, SiF^aF^b). $^{31}P\{^1H\}$ NMR (CD_2Cl_2, 298 K): δ_P 11.4 (d, $^2J_{PP}$ 20.5 Hz, P^1), 3.1 (d, $^2J_{PP}$ 20.5 Hz, P^2).

DFT calculations

Molecular structure optimizations and frequencies calculations were carried out with the Gaussian09 program (revision D.01)[9] using the method B3PW91,[10] including the D3 dispersion correction scheme by Grimme with Becke–Johnson damping.[11] The def2-SVP[12] basis and pseudo potential were used for all atoms and the "ultrafine" grid was employed in all calculations. Stationary points were characterized by vibrational analysis. The structures were optimized in dichloromethane (298 K, 1 atm) using the PCM method.[13] In order to improve the accuracy of the calculated energies, single point energy calculations were carried out on the optimized structures of intermediates and transition states using the method M06,[14] the def2-TZVP[12] basis and pseudo potentials, where appropriate, and the SMD model[15] for the solvent (dichloromethane). Finally a correction of +1.89 kcal mol^{-1} to Gibbs free energy was also applied for the change of the standard state from gas phase (1 atm) to solution (1 M) at 298 K.[16] Delocalization indexes (DI) were calculated using Multiwfn.[17]

Crystal structure determination

Single crystals of SiNP and 7BF_4 were obtained by slow evaporation of dicholoromethane solutions of the compounds; single crystals of **1**PF_6 and **4**PF_6 were grown by slow diffusion of hexane into a THF (**4**PF_6) or dichloromethane solution (**1**PF_6) of the compounds. X-ray diffraction data were collected at 100 (2) K on a Bruker APEX SMART (**1**PF_6, **4**PF_6, 7BF_4) or APEX DUO (SiNP) diffractometer with graphite-monochromated Mo-Kα radiation (λ = 0.71073 Å) using 0.6° ω rotations. Intensities were integrated and corrected for absorption effects with SAINT–PLUS[18] and SADABS[19] programs, both included in APEX2 package. The structures were solved by the Patterson method with SHELXS-97[20] and refined by full matrix least-squares on F^2 with SHELXL-2014[21] under WinGX.[22]

Crystal data for SiNP

$C_{40}H_{40}N_2P_2Si$, 638.77 g mol^{-1}, monoclinic, $P21/c$, a = 23.093(3) Å, b = 9.0864(13) Å, c = 17.039(2) Å, β = 107.176(2)°, V = 3415.9 (8) $Å^3$, Z = 4, reflections collected/independent 65 969/6980 [R(int) = 0.0406], R_1 = 0.0435 [$I > 2\sigma(I)$], wR_2 = 0.1380 (all data). CCDC deposit number 2155640.†

Crystal data for 1PF_6

$2C_{50}H_{58}F_6IrN_4P_3Si{\cdot}CH_2Cl_2{\cdot}C_6H_{14}$, 2455.50 g mol^{-1}, triclinic, $P\bar{1}$, a = 10.9615(7) Å, b = 12.7205(8) Å, c = 20.4705(12) Å, α = 86.1880(10)°, β = 77.4030(10)°, γ = 85.9510(10)°, V = 2774.8(3) $Å^3$, Z = 1, reflections collected/independent 34 093/11 291

[R(int) = 0.0280], R_1 = 0.0293 [$I > 2\sigma(I)$], wR_2 = 0.0762 (all data). CCDC deposit number 2155643.†

Crystal data for $4PF_6$

$4C_{50}H_{57}ClF_6IrN_4P_4Si{\cdot}3C_4H_8O$, 4922.88 g mol^{-1}, monoclinic, $C2/c$, a = 46.824(5) Å, b = 10.9773(11) Å, c = 25.668(3) Å, β = 121.1930(10)°, V = 11 286(2) Å^3, Z = 2, reflections collected/independent 58 271/12 421 [R(int) = 0.0495], R_1 = 0.0364 [$I > 2\sigma(I)$], wR_2 = 0.0815 (all data). CCDC deposit number 2155642.†

Crystal data for $7BF_4$

$C_{50}H_{60}BF_6IrN_4P_2Si{\cdot}CH_2Cl_2$, 1208.98 g mol^{-1}, monoclinic, $P2_1/c$, a = 16.3517(10) Å, b = 11.6078(7) Å, c = 28.9040(17) Å, β = 93.8810(10)°, V = 5473.6(6) Å^3, Z = 4, reflections collected/independent 61 703/11 193 [R(int) = 0.0364], R_1 = 0.0231 [$I > 2\sigma(I)$], wR_2 = 0.0525 (all data). CCDC deposit number 2155641.†

Conflicts of interest

There are no conflicts to declare.

Acknowledgements

Financial support from the Spanish Ministerio de Ciencia e Innovación MCIN/AEI/10.13039/501100011033, under the Project PID2019-103965GB-I00, and the Departamento de Ciencia, Universidad y Sociedad del Conocimiento del Gobierno de Aragón (group E42_20R) is gratefully acknowledged.

Notes and references

1 V. Passarelli, J. J. Pérez-Torrente and L. A. Oro, *Dalton Trans.*, 2016, **45**, 951–962.

2 (*a*) B. S. Mitchell, W. Kaminsky and A. Velian, *Inorg. Chem.*, 2021, **60**, 6135–6139; (*b*) A. Aloisi, É. Crochet, E. Nicolas, J.-C. Berthet, C. Lescot, P. Thuéry and T. Cantat, *Organometallics*, 2021, **40**, 2064–2069; (*c*) J. A. Kephart, A. C. Boggiano, W. Kaminsky and A. Velian, *Dalton Trans.*, 2020, **49**, 16464–16473; (*d*) H. Zhang, G. P. Hatzis, C. E. Moore, D. A. Dickie, M. W. Bezpalko, B. M. Foxman and C. M. Thomas, *J. Am. Chem. Soc.*, 2019, **141**, 9516–9520; (*e*) J. A. Kephart, B. S. Mitchell, A. Chirila, K. J. Anderton, D. Rogers, W. Kaminsky and A. Velian, *J. Am. Chem. Soc.*, 2019, **141**, 19605–19610; (*f*) K. M. Gramigna, D. A. Dickie, B. M. Foxman and C. M. Thomas, *ACS Catal.*, 2019, **9**, 3153–3164; (*g*) M. L. Bin Ismail and C.-W. So, *Chem. Commun.*, 2019, **55**, 2074–2077; (*h*) B. A. Barden, G. Culcu, J. P. Krogman, M. W. Bezpalko, G. P. Hatzis, D. A. Dickie, B. M. Foxman and C. M. Thomas, *Inorg. Chem.*, 2019, **58**, 821–833; (*i*) A. J. Ayres, A. J. Wooles, M. Zegke, F. Tuna and S. T. Liddle, *Inorg. Chem.*, 2019, **58**, 13077–13089; (*j*) H. Zhang, B. Wu, S. L. Marquard, E. D. Litle, D. A. Dickie, M. W. Bezpalko, B. M. Foxman and C. M. Thomas, *Organometallics*, 2017, **36**, 3498–3507; (*k*) G. Culcu, D. A. Iovan, J. P. Krogman, M. J. T. Wilding, M. W. Bezpalko, B. M. Foxman and C. M. Thomas, *J. Am. Chem. Soc.*, 2017, **139**, 9627–9636; (*l*) F. Völcker and P. W. Roesky, *Dalton Trans.*, 2016, **45**, 9429–9435; (*m*) R. W. Carlsen and D. H. Ess, *Dalton Trans.*, 2016, **45**, 9835–9840; (*n*) W. K. Walker, B. M. Kay, S. A. Michaelis, D. L. Anderson, S. J. Smith, D. H. Ess and D. J. Michaelis, *J. Am. Chem. Soc.*, 2015, **137**, 7371–7378; (*o*) W. K. Walker, D. L. Anderson, R. W. Stokes, S. J. Smith and D. J. Michaelis, *Org. Lett.*, 2015, **17**, 752–755; (*p*) F. Völcker, F. M. Mück, K. D. Vogiatzis, K. Fink and P. W. Roesky, *Chem. Commun.*, 2015, **51**, 11761–11764; (*q*) J. P. Krogman, B. M. Foxman and C. M. Thomas, *Organometallics*, 2015, **34**, 3159–3166.

3 Selected references for PNNP: (*a*) A. Prades, S. Núñez-Pertíñez, A. Riera and X. Verdaguer, *Chem. Commun.*, 2017, **53**, 4605–4608; (*b*) F. Trentin, A. M. Chapman, A. Scarso, P. Sgarbossa, R. A. Michelin, G. Strukul and D. F. Wass, *Adv. Synth. Catal.*, 2012, **354**, 1095–1104; (*c*) S. W. Hunt, V. Nesterov and M. G. Richmond, *J. Mol. Struct.*, 2012, **1010**, 91–97; (*d*) L. E. Bowen, M. Charernsuk, T. W. Hey, C. L. McMullin, A. G. Orpen and D. F. Wass, *Dalton Trans.*, 2010, **39**, 560–567; (*e*) B. R. Aluri, N. Peulecke, B. H. Müller, S. Peitz, A. Spannenberg, M. Hapke and U. Rosenthal, *Organometallics*, 2010, **29**, 226–231; (*f*) P. Fonteh and D. Meyer, *Metallomics*, 2009, **1**, 427–433; (*g*) J. Bravo, J. Castro, S. García-Fontán, M. C. Rodríguez-Martínez, G. Albertin, S. Antoniutti and A. Manera, *J. Organomet. Chem.*, 2007, **692**, 5481–5491.

4 Selected references of PNP: (*a*) M. Rodriguez-Zubiri, V. Gallo, J. Rosé, R. Welter and P. Braunstein, *Chem. Commun.*, 2008, 64–66; (*b*) L.-C. Song, X.-F. Han, W. Chen, J.-P. Li and X.-Y. Wang, *Dalton Trans.*, 2017, **46**, 10003–10013; (*c*) L.-C. Song, L.-D. Zhang, W.-W. Zhang and B.-B. Liu, *Organometallics*, 2018, **37**, 1948–1957; (*d*) S. A. Bartlett, J. Moulin, M. Tromp, G. Reid, A. J. Dent, G. Cibin, D. S. McGuinness and J. Evans, *Catal. Sci. Technol.*, 2016, **6**, 6237–6246; (*e*) A. M. Lifschitz, N. A. Hirscher, H. B. Lee, J. A. Buss and T. Agapie, *Organometallics*, 2017, **36**, 1640–1648; (*f*) S. Orgué, T. León, A. Riera and X. Verdaguer, *Org. Lett.*, 2015, **17**, 250–253; (*g*) C. Mu, J. He, S. Lü, J. Yang, Y. Xie, K. Hu, P. Yan and Y.-L. Li, *Polyhedron*, 2021, **200**, 115087; (*h*) S. Todisco, V. Gallo, P. Mastrorilli, M. Latronico, N. Re, F. Creati and P. Braunstein, *Inorg. Chem.*, 2012, **51**, 11549–11561; (*i*) S. Naik, J. T. Mague and M. S. Balakrishna, *Inorg. Chim. Acta*, 2013, **407**, 139–144.

5 (*a*) M. L. Clarke, A. M. Z. Slawin and J. D. Woolins, *Phosphorus, Sulfur Silicon Relat. Elem.*, 2001, **168–169**, 329–332; (*b*) S. M. Aucott, M. L. Clarke, A. M. Z. Slawin and J. D. Woolins, *J. Chem. Soc., Dalton Trans.*, 2001, 972–976.

6 (*a*) V. Passarelli and F. Benetollo, *Inorg. Chem.*, 2011, **50**, 9958–9967; (*b*) V. Passarelli, J. J. Pérez-Torrente and

L. A. Oro, *Dalton Trans.*, 2015, **44**, 18596–18606; (*c*) V. Passarelli, J. J. Pérez-Torrente and L. A. Oro, *Inorg. Chem.*, 2014, **53**, 972–980.

7 (*a*) M. Zhong, J. Wei, W.-X. Zhang and Z. Xi, *Organometallics*, 2021, **40**, 310–313; (*b*) X. Xin and C. Zhu, *Dalton Trans.*, 2020, **49**, 603–607; (*c*) L.-C. Song, X.-Y. Yang, X.-Y. Gao and M. Cao, *Inorg. Chem.*, 2019, **58**, 39–42; (*d*) G. Feng, M. Zhang, P. Wang, S. Wang, L. Maron and C. Zhu, *Proc. Natl. Acad. Sci. U. S. A.*, 2019, **116**, 17654–17658; (*e*) J. Ji, F. Wu, L.-M. Shi, A.-Q. Jia and Q.-F. Zhang, *J. Organomet. Chem.*, 2019, **885**, 1–6; (*f*) A. A. Kassie, P. Duan, E. T. McClure, K. Schmidt-Rohr, P. M. Woodward and C. R. Wade, *Inorg. Chem.*, 2019, **58**, 3227–3236; (*g*) A. A. Kassie, P. Duan, M. B. Gray, K. Schmidt-Rohr, P. M. Woodward and C. R. Wade, *Organometallics*, 2019, **38**, 3419–3428; (*h*) S. Khan, S. Pal, N. Kathewad, I. Purushothaman, S. De and P. Parameswaran, *Chem. Commun.*, 2016, **52**, 3880–3882; (*i*) A. Alzamly, S. Gambarotta and I. Korobkov, *Organometallics*, 2013, **32**, 7107–7115; (*j*) S. Zhang, R. Pattacini and P. Braunstein, *Dalton Trans.*, 2011, **40**, 5711; (*k*) S. Zhang, R. Pattacini and P. Braunstein, *Organometallics*, 2010, **29**, 6660–6667.

8 J. Clayden, *Organic chemistry*, Oxford University Press, Oxford, 2005. ISBN 978-0-19-850346-0.

9 M. J. Frisch, G. W. Trucks, H. B. Schlegel, G. E. Scuseria, M. A. Robb, J. R. Cheeseman, G. Scalmani, V. Barone, B. Mennucci, G. A. Petersson, H. Nakatsuji, M. Caricato, X. Li, H. P. Hratchian, A. F. Izmaylov, J. Bloino, G. Zheng, J. L. Sonnenberg, M. Hada, M. Ehara, K. Toyota, R. Fukuda, J. Hasegawa, M. Ishida, T. Nakajima, Y. Honda, O. Kitao, H. Nakai, T. Vreven, J. A. Montgomery Jr., J. E. Peralta, F. Ogliaro, M. Bearpark, J. J. Heyd, E. Brothers, K. N. Kudin, V. N. Staroverov, R. Kobayashi, J. Normand, K. Raghavachari, A. Rendell, J. C. Burant, S. S. Iyengar, J. Tomasi, M. Cossi, N. Rega, J. M. Millam, M. Klene, J. E. Knox, J. B. Cross, V. Bakken, C. Adamo, J. Jaramillo, R. Gomperts, R. E. Stratmann, O. Yazyev, A. J. Austin, R. Cammi, C. Pomelli, J. W. Ochterski, R. L. Martin, K. Morokuma, V. G. Zakrzewski, G. A. Voth, P. Salvador, J. J. Dannenberg, S. Dapprich, A. D. Daniels, C. Farkas, J. B. Foresman, J. V. Ortiz, J. Cioslowski and D. J. Fox, *Gaussian 09, Revision D.01*, Gaussian, Inc., Wallingford CT, 2009.

10 J. P. Perdew, in *Electronic Structure of Solids '91*, Ed. P. Ziesche and H. Eschrig, Akademie Verlag, Berlin, 1991.

11 S. Grimme, S. Ehrlich and L. Goerigk, *J. Comput. Chem.*, 2011, **32**, 1456–1465.

12 F. Weigend and R. Ahlrichs, *Phys. Chem. Chem. Phys.*, 2005, **7**, 3297–3305.

13 J. Tomasi, B. Mennucci and R. Cammi, *Chem. Rev.*, 2005, **105**, 2999–3093.

14 Y. Zhao and D. G. Truhlar, *J. Chem. Phys.*, 2006, **125**, 194101.

15 A. V. Marenich, C. J. Cramer and D. G. Truhlar, *J. Phys. Chem. B*, 2009, **113**, 6378–6396.

16 V. S. Bryantsev, M. S. Diallo and W. A. Goddard III, *J. Phys. Chem. B*, 2008, **112**, 9709–9719.

17 T. Lu and F. Chen, *J. Comput. Chem.*, 2012, **33**, 580–592.

18 *SAINT+: Area-Detector Integration Software, version 6.01*, Bruker AXS, Madison, WI, 2001.

19 G. M. Sheldrick, *SADABS program*, University of Göttingen, Göttingen, Germany, 1999.

20 G. M. Sheldrick, *SHELXS 97, Program for the Solution of Crystal Structure*, University of Göttingen, Göttingen, Germany, 1997.

21 G. M. Sheldrick, *Acta Crystallogr., Sect. C: Struct. Chem.*, 2015, **71**, 3–8.

22 L. J. Farrugia, *J. Appl. Crystallogr.*, 2012, **45**, 849–854.